Publ. Natl. Astron. Obs. Japan Vol. 9. 21–53 (2006)

Tolerance Test of a Sample Filter for Use in Space

Masao HAYASHI[1], Mikito TANAKA[1], Yutaka KOMIYAMA, Sadanori OKAMURA[1],
Saku TSUNETA, Motokazu NOGUCHI, Masao NAKAGIRI,
Ryouhei KANO, and Toshihiko KIMURA[2]
(Received October 31, 2005)

Abstract

We report the result of a tolerance test of a sample filter for the planned Very Wide Field Imager on board the Hubble Origin Probe. We investigated whether the properties of the filter and its components, i.e., color glass, synthetic quartz, short-wavelength-pass coating and long-wavelength-pass coating, changed after they were put in a vacuum, after they were subjected to a thermal cycle, and after they were exposed to γ ray. Results are shown mostly in graphical form. No significant change of the properties was observed for the filter and any of the components before and after the tests, except for the color glass which was exposed to strong γ ray.

Key words: filter test; vacuum; thermal cycle; γ ray exposure; Hubble Origin Probe (HOP)

1. Introduction

The proposed Hubble Origins Probe (HOP) is a 2.4m space telescope which will be launched in 2010 as the successor of the Hubble Space Telescope (HST). HOP is a no-new-technology HST-class observatory with a much lighter unaberrated mirror and optical telescope assembly than those in HST. The Cosmic Origin Spectrograph (COS) and the Wide Field Camera 3 (WFC3), both were developed for HST, are supposed to be the core instruments of HOP. Japanese partners of the HOP proposal are leading the development of a high-throughput, Very Wide Field Imager (VWFI) that achieves a field of view approximately 20 times larger than the Advances Camera for Surveys (ACS) of HST.

VWFI covers a half of the unaberrated focal plane with CCD mosaic. A few filter wheels will be installed. For VWFI, we will use broad band filters whose bandpasses are defined by a short-wavelength-pass (hereafter 'high-pass') interference coating and a long-wavelength-pass (hereafter 'low-pass') interference coating with the help of appropriate color glass.

In order to investigate whether the filters to be used for VWFI are robust in space conditions, we carried out a tolerance test of a filter and its components, i.e., color glass, synthetic quartz, high-pass coating and low-pass coating.

We chose the z_R filter, the reddest one among our possible choice of VWFI filters, as the target of the present test because it is regarded as least robust among the filters of our possible choice. The reasons are:

- Both the high-pass and the low-pass interference coatings have the same structure, i.e., the same sequence, of evaporation layers of materials.
- The coating is thicker for redder wavelengths than for bluer wavelengths, and for a given cut-off wavelength, the high-pass coating is thicker than the low-pass coating.
- Secular time variation of the transmission curve due to humidity, that is, shift toward redder wavelength under a highly humid environment, is larger for thicker coatings, if the layer structure is the same.
- Thicker coatings are subject to higher risk of peeling off.

The sample used for the test was provided by Asahi Spectra, Co. Ltd., which consisted of five equivalent sets of glasses of 50mm×50mm. Each of the five sets consisted of four pieces, a z_R filter (ZR), a color glass RG695 (RG), synthetic quartz with low-pass coating LWP9500Å on a side (LWP), and synthetic quartz with high-pass coating SWP10500Å on a side (SWP). The z_R filter is made of RG, LWP, and SWP bonded together. The bond is the same as the one which is used for the filters of Suprime-Cam (Miyazaki et al. 2002) and FOCAS(Kashikawa et al. 2002) of Subaru Telescope (Kaifu et al. 2000; Iye et al. 2004). Detailed description of the four pieces are given below and their pictures are shown in figure 1.

1. ZR
   size: 50mm × 50mm × 6mm
   material: LWP9500Å*synthetic quartz + (bond) + RG695 + (bond) + synthetic quartz*SWP10500Å
   (* represents deposition.)
2. RG
   size: 50mm × 50mm × 2mm

[1]Department of Astronomy, school of Science, University of Tokyo
[2]ASAHI SPECTRA CO. LTD

material: Schott RG695 color glass
No coating on either side.

3. LWP
size: 50mm × 50mm × 2mm
material: LWP9500Å*synthetic quartz
Coating on one side.

4. SWP
size: 50mm × 50mm × 2mm
material: SWP10500Å*synthetic quartz
Coating on one side.

2. Method of the Test

The sample pieces were subjected to the three tests, vacuum test, thermal cycle test, and radiation test. Table 1 summarizes which tests were applied to the five sets of test pieces. The set No.1 was not subjected to any test so that it was used as the reference. After each test, we made an eyeball inspection and a tape check, and then we measured the transmission curve to compare it with 'the default transmission curve', which were measured for all the 20 pieces of the sample in advance of the tests. The tape check is a test to see if the coating peels off easily. We stuck a piece of plastic tape (Scotch mending tape: 810-1-12) on the coating of the test piece and peeled off the tape to examine the tape and the surface of the piece.

The spectrometer used in the present study was UV-3100PC manufactured by Shimazu Co. Ltd. Transmission of a test piece was measured over the wavelength range of 300nm–1200nm. Throughout the test, we used the slit width of 0.5nm and the sampling pitch of 0.5nm. The detector of UV-3100PC can be changed automatically between the optical detector and the infrared detector at a user-specified wavelength, which was set at 890nm in the present test.

In order to assess the stability of the spectrometer and to estimate the error of measurements, the baseline, which is the transmission curve measured without any sample in the spectrometer, was measured at the beginning of each of the bunches of consecutive measurements. The baseline measured in advance of the tests, together with the default transmission curve, is referred to as the 'default baseline'. During the measurment of the default transmission curve and the default baseline, the temperature was 29°C and the humidity was 66%.

2.1 Vacuum Test

We carried out a vacuum test on 3 to 8 August, 2005. The vacuum chamber used is TD2001-C manufactured by Power Supply Osaka Vacuum, Co. Ltd. We put the pieces of ZR, RG, LWP, and SWP in the four sets, Nos. 2, 3, 4 and 5, into the vacuum chamber at 15:30, 3 August 2005, and kept the chamber vacuum for 114.5 hours. The degree of vacuum in the chamber during the test period was 3.1 – 3.2 $\times 10^{-7}$ torr. We took the pieces out of the chamber at 10:00, 8 August 2005. The pieces were subjected to the eyeball inspection and the tape check, and then their transmission curves were measured. The temperature was 28°C and the humidity was 67% during the measurment.

2.2 Thermal Cycle Test

The temperature in the chamber was changed from –30°C to 85°C. The number of thermal cycles was ten in the first test and twenty-five in the second test. In order to prevent the humidity in the chamber from going up considerably, dry nitrogen was flowed into the chamber at a rate of 10 litter a minute, and the temperature was changed slowly. The details of the thermal cycle are as follows:

1. Raise the temperature from room temperature to 85°C in 4 hours.
2. Keep the temperature at 85°C for an hour.
3. Lower the temperature from 85°C to –30°C in an hour.
4. Keep the temperatuere at –30°C for an hour.
5. Raise the temperature from –30°C to 85°C in four hours.
6. Keep the temperatuere at 85°C for an hour.
7. Repeat (3) to (6) nine times or twenty-four times.
8. Lower the temperature to room temperature in an hour.

Figure 3 shows the variation of the temperature and humidity during the thermal cycle tests.

After the tests, the pieces were subjected to the eyeball inspection and the tape check, and then their transmission curves were measured. The temperature and the humidity during the mesurements were 27°C and 71% and 27°C and 68% in the first and the second tests, respectively.

2.3 Radiation Test

We carried out a radiation test, total dose test, on 17 to 18 August, 2005. We used the cobalt60 γ ray source at the Tokyo Metropolitan Industrial Technology Research Institute.

The pieces of set Nos. 2, 3, and 4 were subjected to the test. We set up the filter stands at two differnt distances from the γ ray source and irradiate γ ray for five hours. The pieces on the stand near to the source, No. 2, were exposed to a total of 10 krad of γ ray, which corresponds to

No.	Vacuum	Thermal Cycle (10+25 cycles)	Radiation 5 krad	Radiation 10 krad
Set-1		(used as the reference)		
Set-2	○			○
Set-3	○		○	
Set-4	○	○	○	
Set-5	○	○		

Table 1: Summary of the tests applied to the five sets of test pieces.

the amount of on-orbit exposure for about ten years, while those on the stand far to the source, Nos. 3 and 4, were exposed to 5 krad of irradiation. The irradiation rate is based on the value calculated at the Institute on 17 August, and its accuracy is about 10%. Figure 4 shows the layout of the radiation test.

After the tests, the pieces were subjected to the eyeball inspection and the tape check, and then their transmission curves were measured. The temperature was 29°C and the humidity was 67 % during the measurement.

3. Result of the Test

The default transmission curves of all the pieces are shown in figure 5 to figure 8. The poor signal-to-noise ratio around 890nm is due to the change of the detectors.

After each test, we measured the transmission curve of the sample piece subjected to the test and compared it with the default curve of the piece. At the same time we also measured the transmission curves of the pieces of Set No.1, which was not subjected to any test, as the reference.

3.1 Estimation of Measurement Error

The error of the measurements in the present tests were estimated from the repeated mesurements of the reference set No.1. We measured the transmission curves of the pieces of set No.1 after each test, though they were not actualy subjected to the test. This is referred to as the calibration measurement. Transmission curve of the calibration mesurement and the corrsponding default transmission curve are always included in the graph of respective tests.

We calculate the difference between the default transmission curve of a piece of set No.1 and that of the same piece in the calibration measurement. The difference was calculated for the four tests, i.e., vacuum test, two thermal cycle tests and radiation test, and the mean and the standard deviation with respect to the four tests were computed. The result is shown in figure 9 for ZR-1 and RG-1. We regard the standard deviation shown in figure 9 as the typical error of the present measurements. It is slightly less than $\pm 1\%$ except at the steep edges of the transmission curve. The error was not properly estimated for LWP and SWP due to the lack of sufficient data. We assume that the errors of LWP and SWP measurements are similar to those of ZR-1 and RG-1.

In order to examine the stability of the spectrometer, we show in figure 10 the difference between the default baseline and the baseline measured after each test. Except for the region of low signal-to-noise at around 850nm–950nm due to the change of the detector, the baseline is found to be very stable at the level of much less than 1%.

3.2 Vacuum Test

The pieces of sets Nos. 2, 3, 4 and 5 were subjected to the vacuum test. The eyeball inspection after the test revealed no problem for all the pieces. All the pieces passed the tape check as well.

The transmission curves of the test pieces measured after the vacuum test are shown by the red curves in figure 11 to figure 14. The respective default curves are also plotted in these figures by the black curves. The difference between the default curve for the pieces of set No. 1 and the transmission measured in the calibration measurement is shown in figure 15. Figure 16 shows, for each of the ZR, RG, LWP, and SWP, the difference of the piece which showed the largest difference among the four sets subjected to the vacuum test.

In figure 16, large differences are seen at the sharp edges of the transmission curve. We regard them insignificant considering that similar large differences are seen in figures 9 and 15. For the rest of part, the differences are all within the error of the measurement which is discussed in section 3.1. Accordingly, we conclude that the differences are all within the error of the measurement and all the pieces of the four sets passed the vacuum test.

3.3 Thermal Cycle Test

The pieces of sets Nos. 4 and 5 were subjected to the thermal cycle test. The eyeball inspection and the tape check after the test revealed no problem for all the pieces.

The transmission curves of the pieces subjected to the second thermal cycle test (25 cycles) are shown by the red curves in figure 17 to figure 20. The respective default curves are also plotted in these figures by the black curves. The difference between the default curve for the pieces of set No. 1 and the transmission measured in the calibration measurement is shown in figure 21. Figure 22 shows, for each of the ZR, RG, LWP, and SWP, the difference of the piece which showed the larger of set No.4 and set No.5. The maximum differences shown in figure 22 are all within the error of the measurement.

The result of the first thermal cycle test is similar to that of the second test. Accordingly, all the pieces of the two sets passed the thermal cycle test.

3.4 Radiation Test

The pieces of sets Nos. 2, 3 and 4 were subjected to the radiation test.; No.2 was exposed to γ ray of 10 krad and Nos. 3 and 4 to 5 krad.

The eyeball inspection and the tape check after the test revealed no problem for all the pieces.

The transmission curves of the test pieces measured after the radiation test are shown by the red curves in figure 23 to figure 26. The respective default curves are also plotted in these figures by the black curves. The difference between the default curve for the pieces of set No. 1 and the transmission measured in the calibration measurement is shown in figure 27.

The difference between the default curve and the transmission measured after the radiation test is shown in figure 28 for RG. In figure 28, the curve of RG-2 shows a slight but significant decrease at around 750nm. Similar trend of decrease is also seen for RG-3 and RG-4 though the significance is marginal. It is noted that figure 28 is corrected for the variation of baseline.

Figure 29 shows, for each of ZR, LWP and SWP, the curve of the piece which showed the largest difference among the three sets, Nos. 2, 3, and 4. All the differences are within errors.

4. Conclusion and Discussion

Table 2 summarizes the results of this test. All the sample pieces passed the vacuum test and the thermal cycle test. In the radiation test, however, RGs showed the decrease of transimission although the significance is marginal for RGs in sets Nos.3 and 4, which were exposed to a total of 5krad of γ ray. The decrease does not seem to be in proportion to the total amount of irradiation, because a half of the decrease in transmission seen in RG of set No.2, if present in RGs in sets Nos. 3 and 4, would be detected considering our small measurement error. It is noted that ZR in set No.2 exposed to 10krad of γ ray did not show significant decrease in transmission. This is probably because the color glass in ZR is covered by synthetic quartz on both sides.

We encountered a problem during this test. After the first thermal test, the transmission of some pieces showed significant decrease. This was later found to be due to the stain on the surface which we did not notice. The record showed that the humidity in the thermostatic chamber had risen up to about 70% once. The stain was probably due to dew condensation. We cleaned the surface of the test pieces and performed the second thermal cycle test. In future experiment, we have to take care of the dew condensation in the thermostatic chamber by examining the critical humidity in the chamber.

The present test demonstrated that the interference coating is robust to γ ray irradiation of up to 10 krad. The red color glass RG 695 is shown affected by 10 krad of γ ray irradiation. It is expected that radiation affects blue color glass more than red color glass. The effects of radiation on various color glasses are to be examined thoroughly (see Nishino et al. 1998).

Acknowledgments

We would like to thank Dr. Taro Sakao of Institute for Space and Astronautical Science, Japan Aerospace Exploration Agency for giving us useful data and advice for the radiation test, and Mr. Noboru Sakurai at Tokyo Metropolitan Industrial Technology Research Institute for practical help in the radiation test.

References

Iye, M. et al. 2004, *PASJ* , **56**, 381.
Kashikawa, N. et al. 2002, *PASJ*, **54**, 819.
Kaifu, N. et al. 2000, *PASJ*, **52**, 1.
Miyazaki, S. et al. 2002, *PASJ*, **54**, 833.
Nishino, Y. et al. 1998, *Publ. NAOJ*, **3**, 145.

No.	Vacuum	Thermal Cycle	Radiation (10 krad)	Radiation (5 krad)
ZR	○	○	○	○
RG	○	○	×	△
LWP	○	○	○	○
SWP	○	○	○	○

Table 2: The results of the tests. ○ means that the component cleared the test.

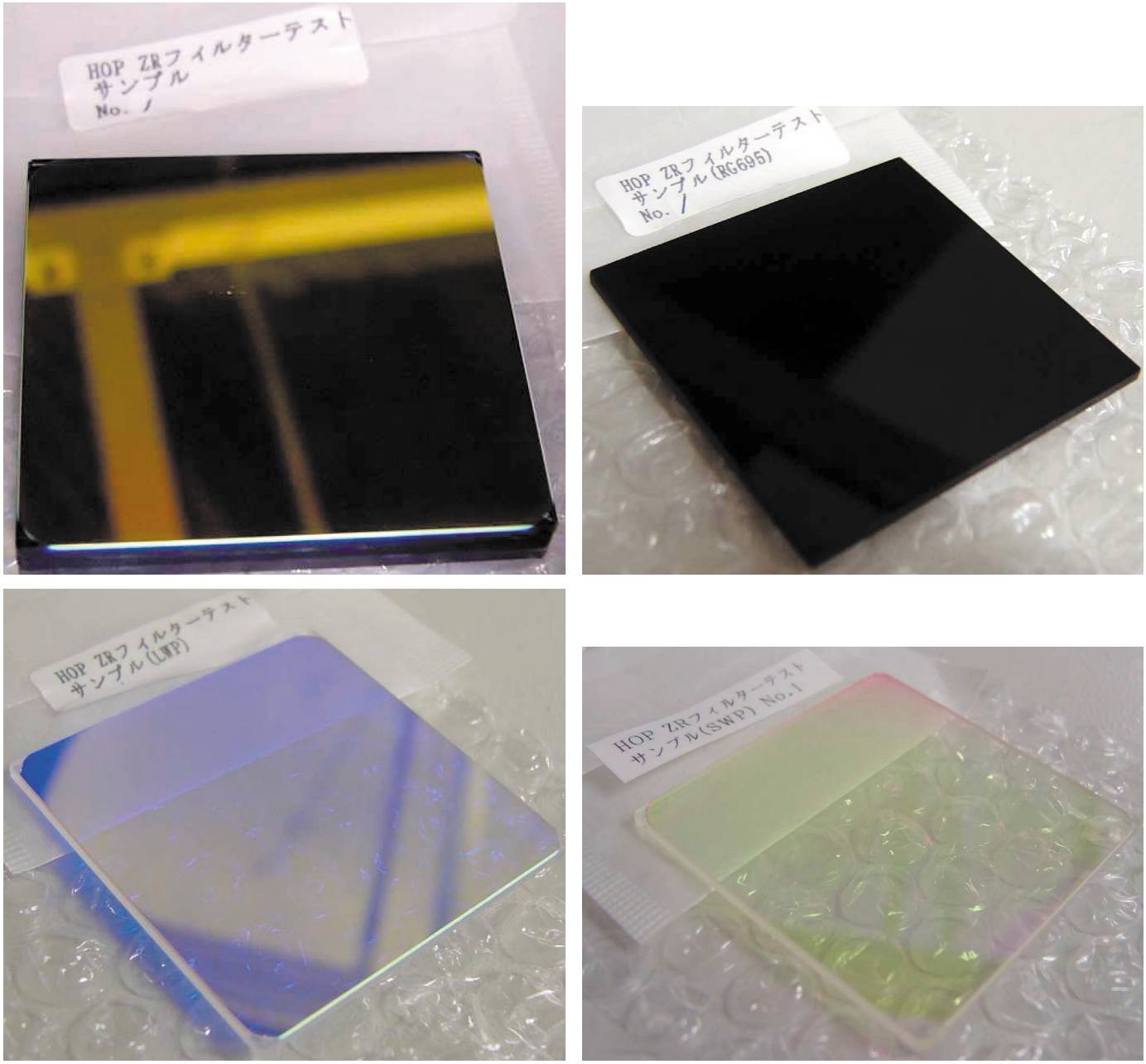

Figure 1: Sample filters of set No.1. The upper left is ZR. The upper right is RG. The lower left is LWP. The lower right is SWP.

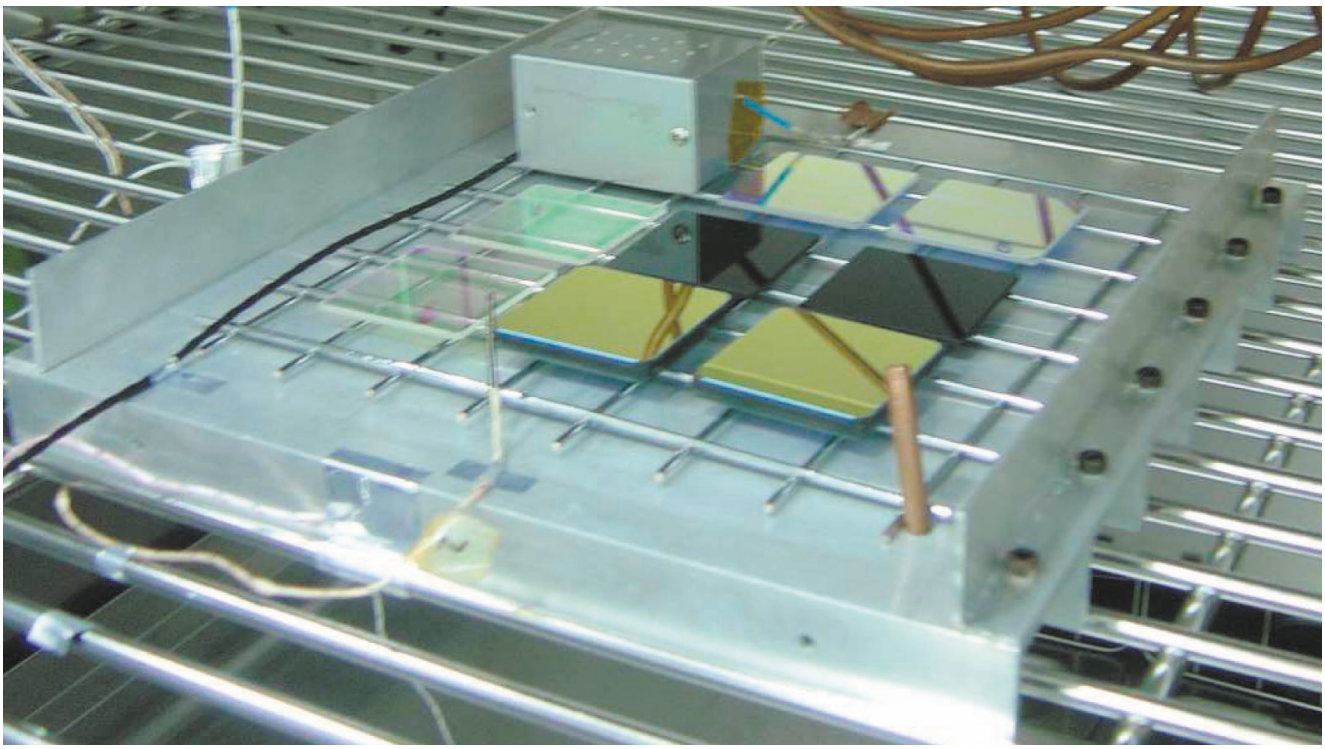

Figure 2: The setting of the pieces in the thermostatic chamber during the thermal cycle tests. During the test, the aluminum table was covered by the lid and dry nitrogen was flowed through the copper tube (seen this side right of the table). The temperature and the humidity were monitored by a thermometer and a hygrometer placed in the small box (seen at the far side).

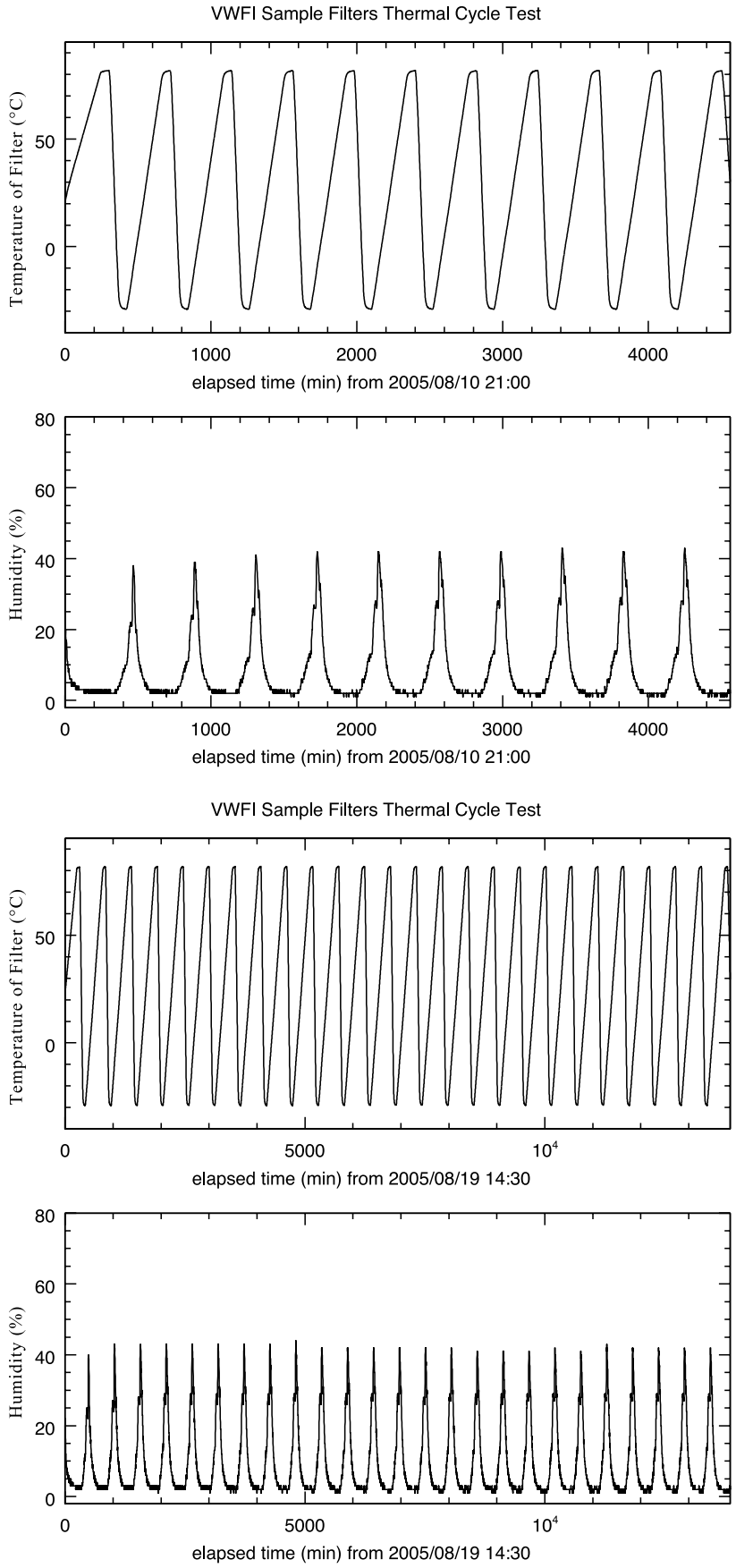

Figure 3: The variation of the temperature and humidity in the thermostatic chamber during the thermal cycle tests. The top two panels are for the first test and the bottom two panels are for the second test.

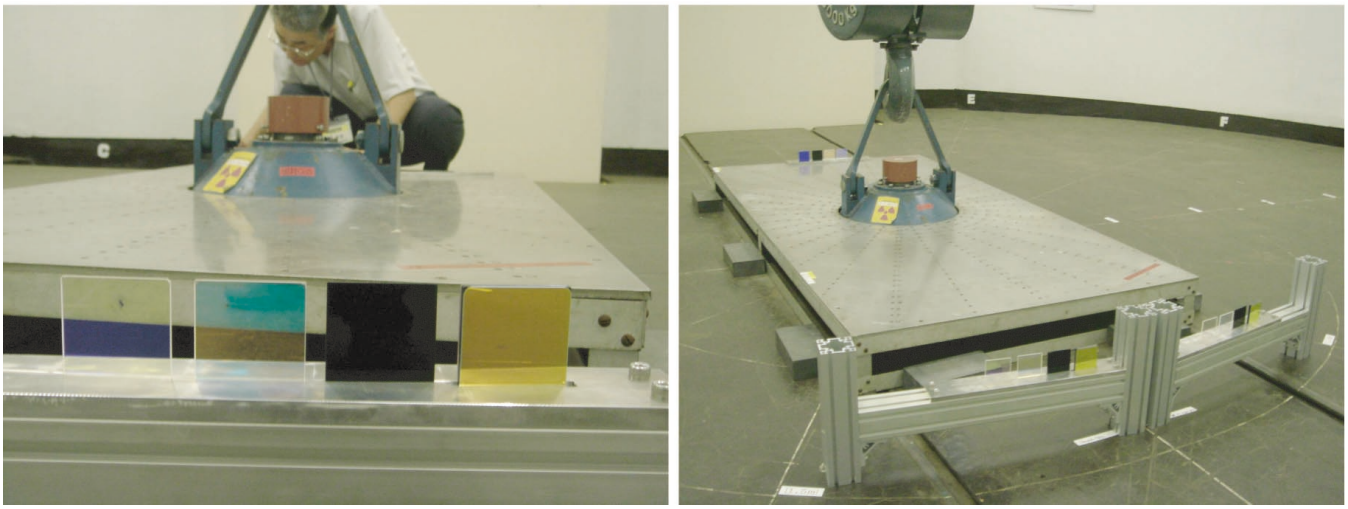

Figure 4: Layout of the sample pieces (SWP,LWP,RG, and ZR from left to right) on the filter stand (left). Layout of the sets in the radiation room (right). Set No.3 is this side left, No.4 is this side right, and No.2 is far side.

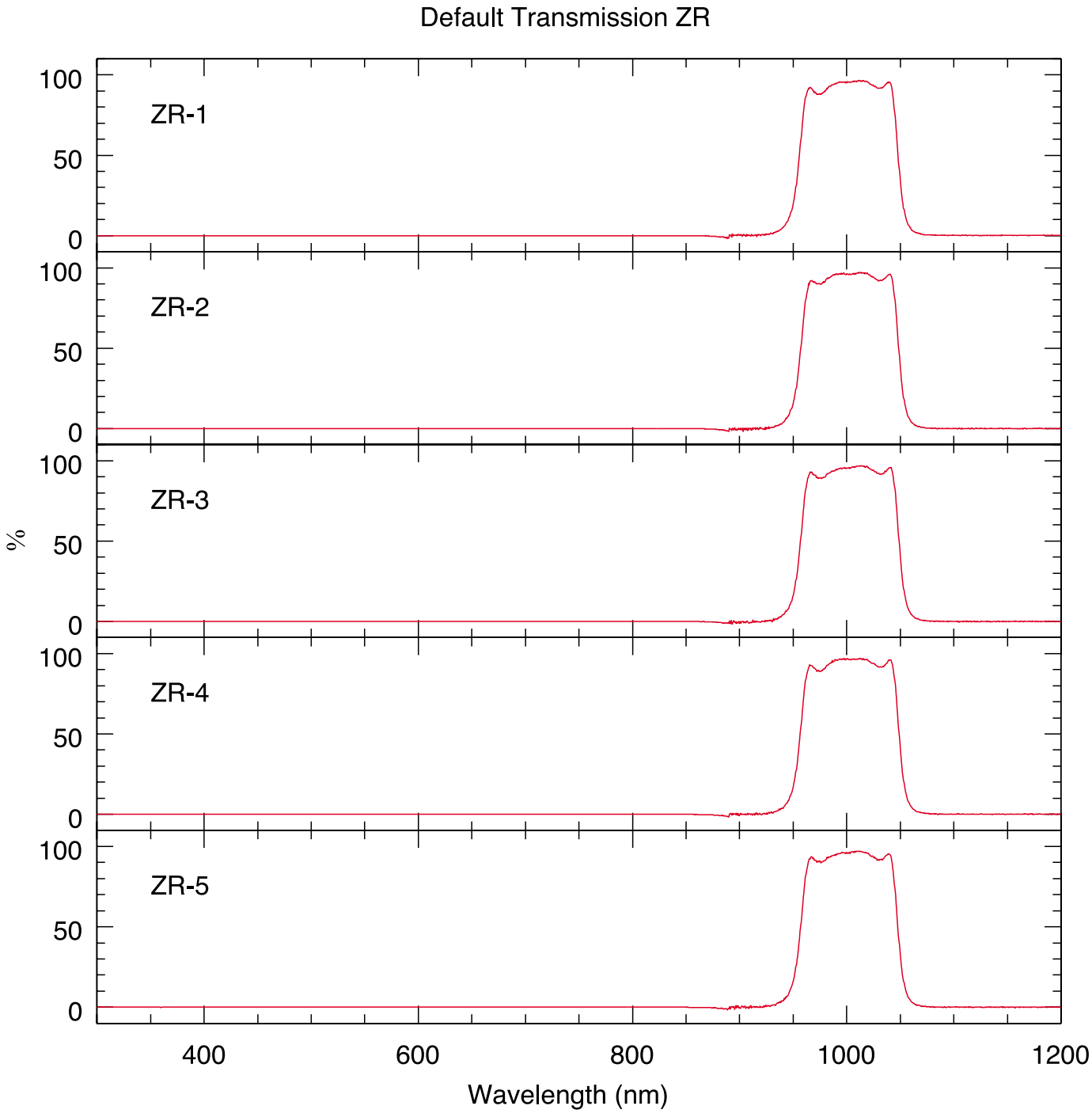

Figure 5: The default transmission curve of ZR.

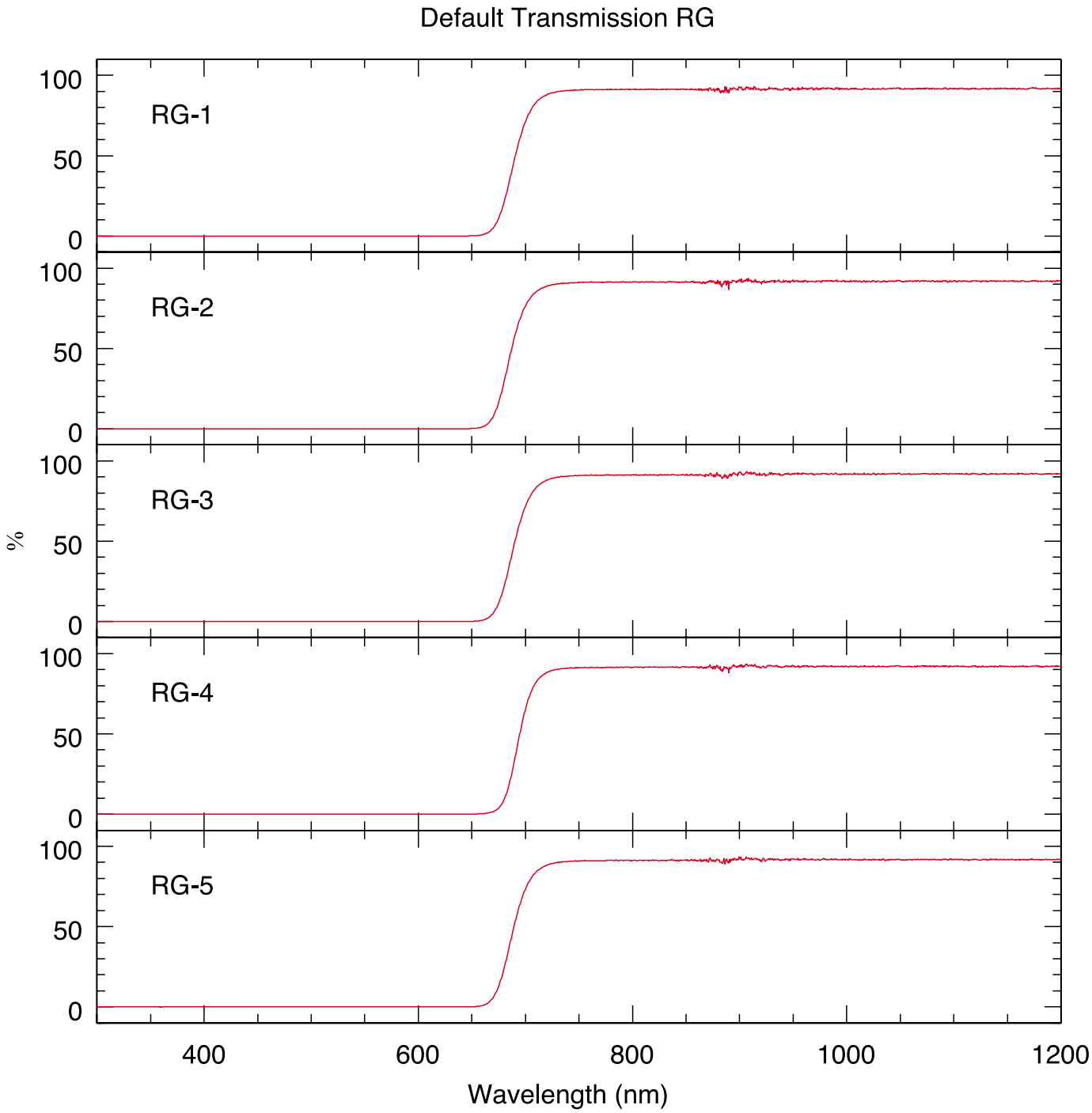

Figure 6: The default transmission curve of RG.

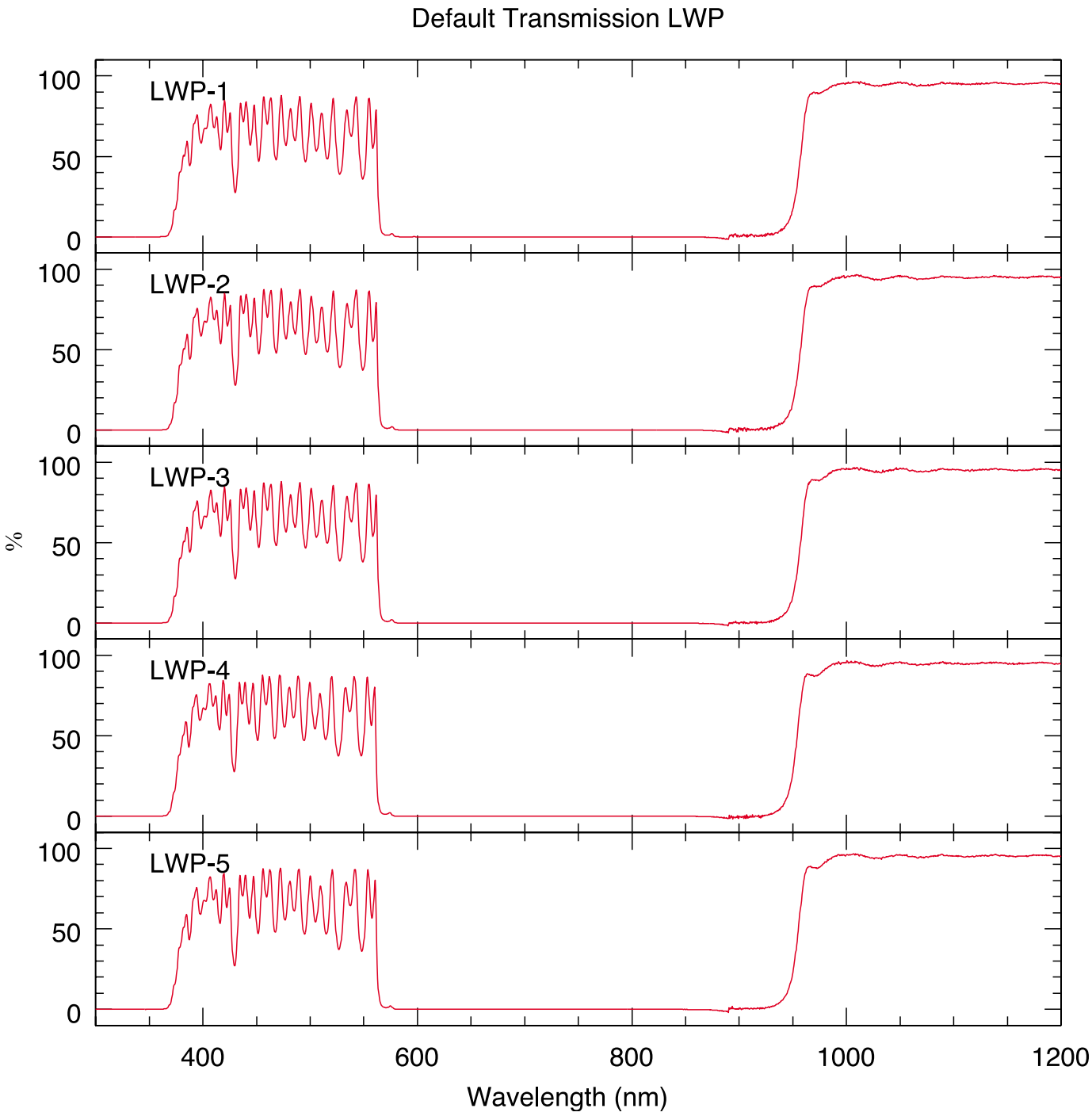

Figure 7: The default transmission curve of LWP.

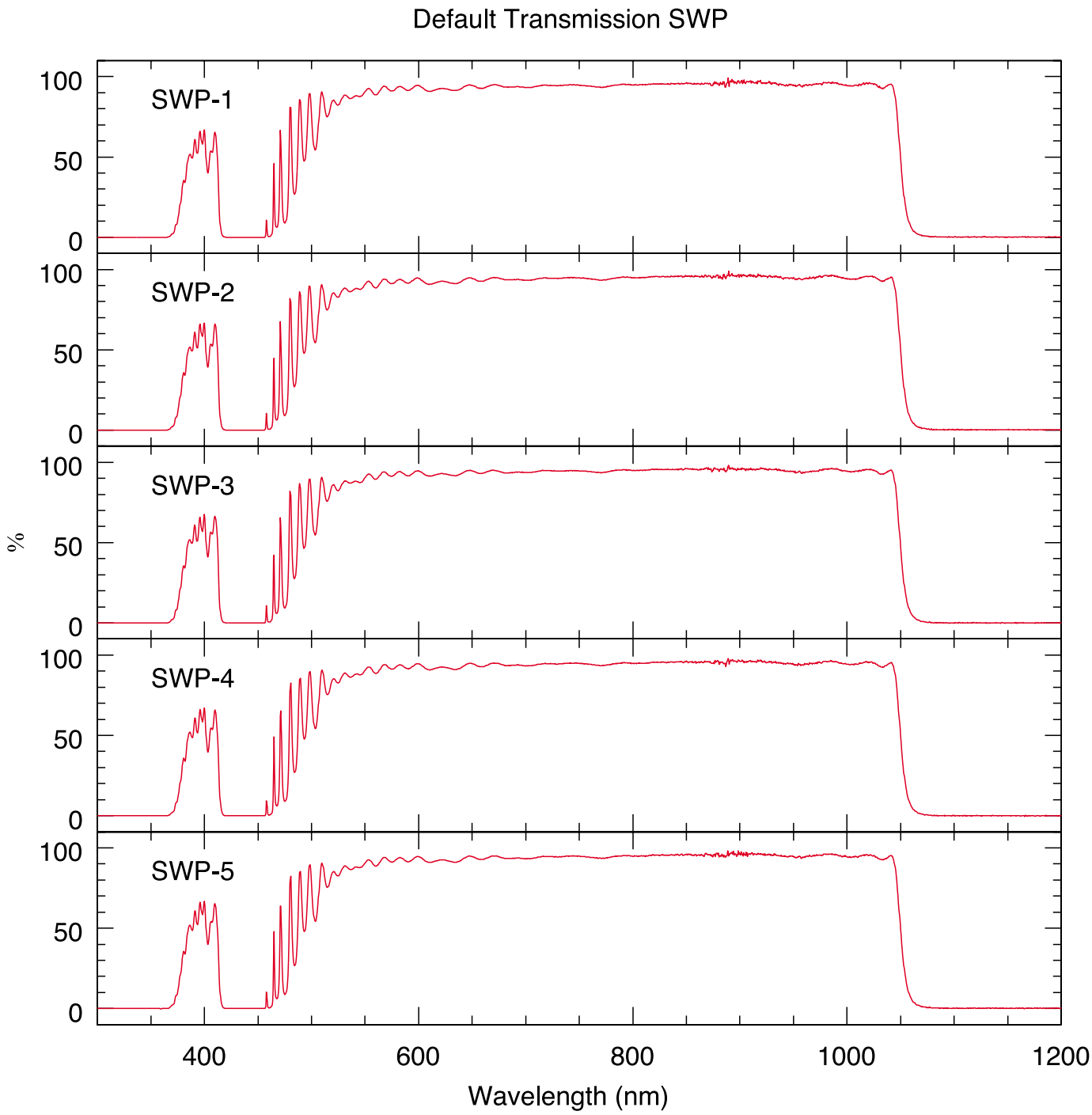

Figure 8: The default transmission curve of SWP.

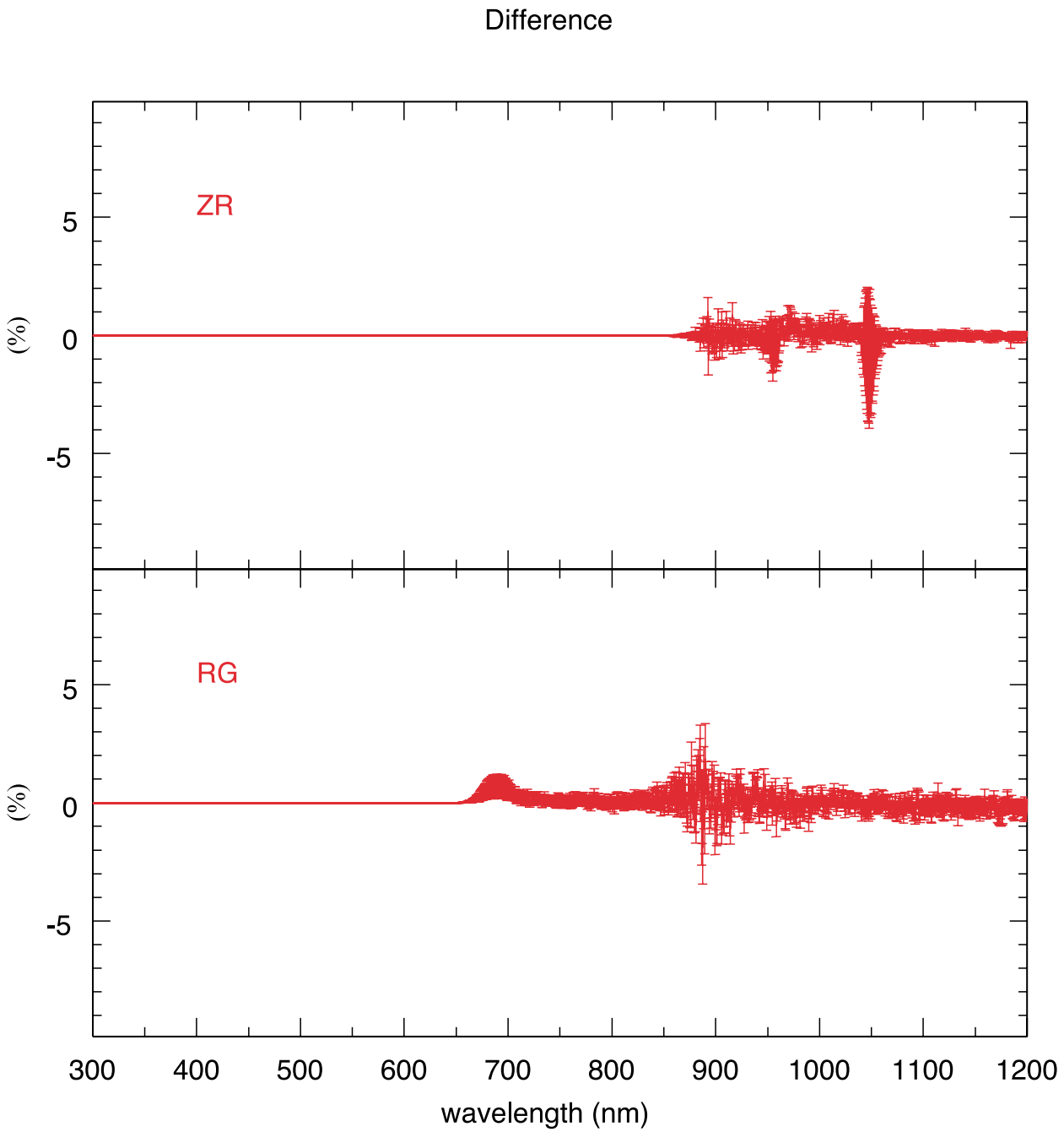

Figure 9: The mean and the standard deviation of the differences between the default transmission curve and the transmission curve measured after the tests for ZR-1 and RG-1.

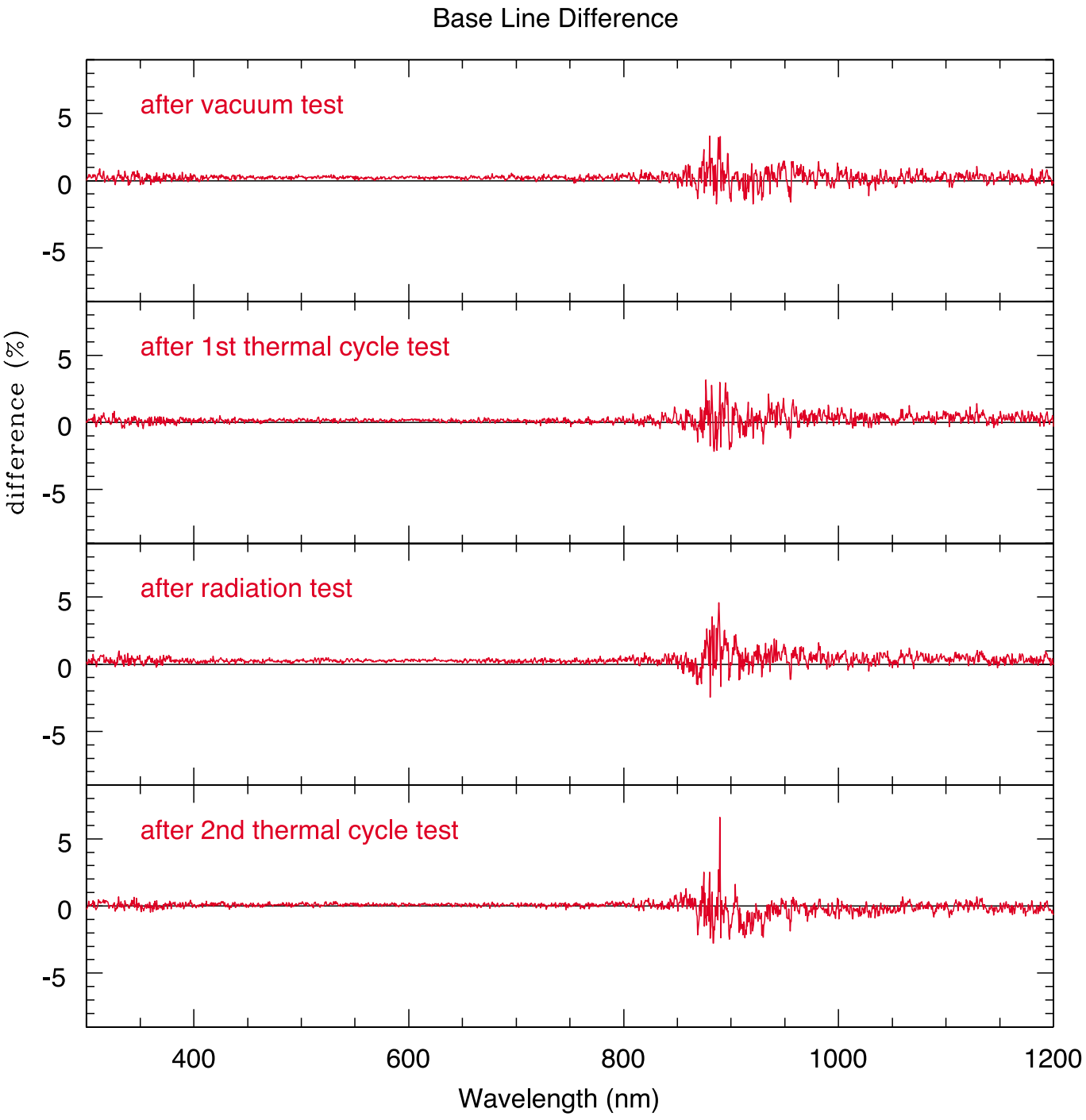

Figure 10: The difference between the default baseline and the baseline after each test.

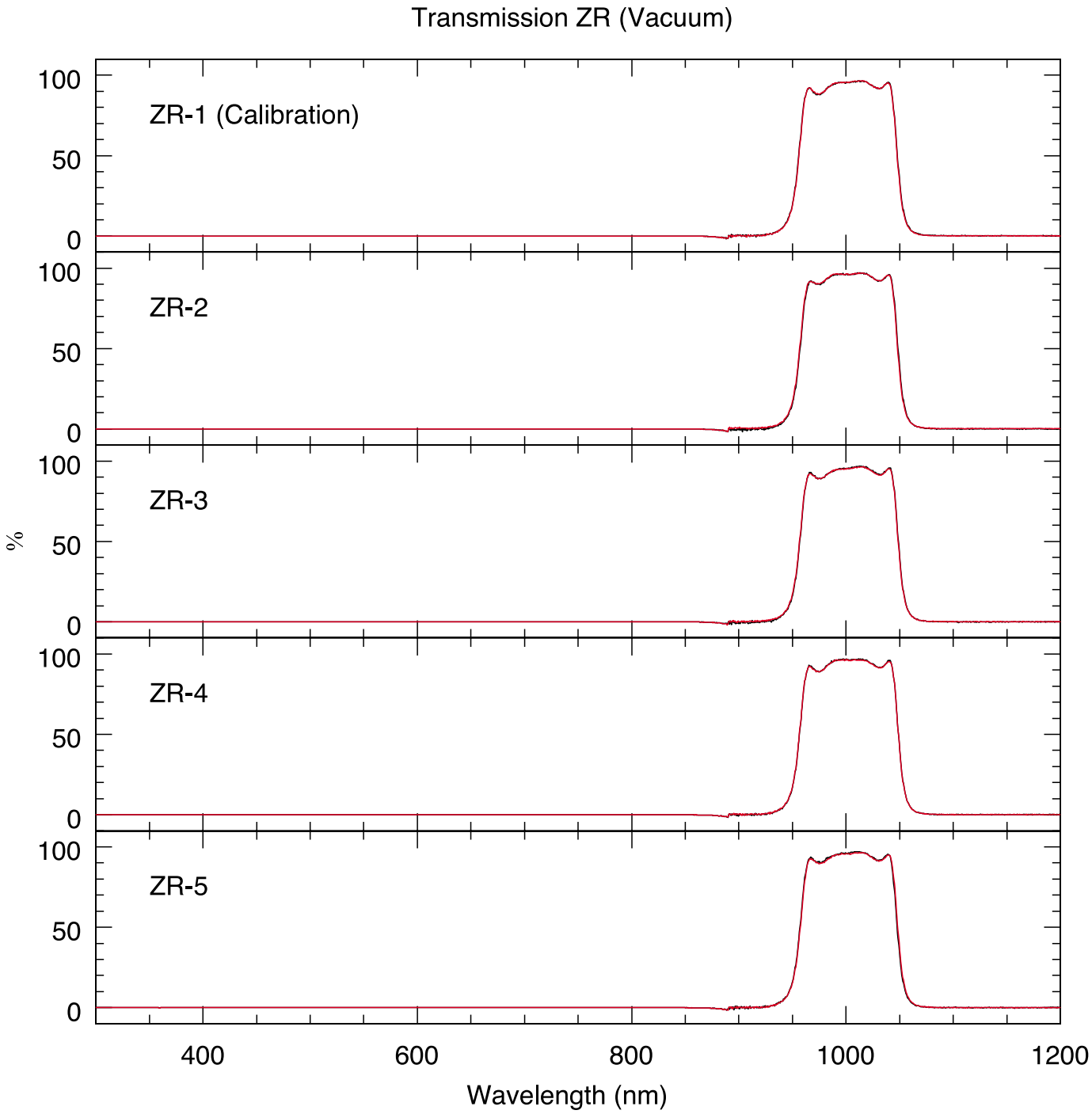

Figure 11: Transmission curves (red) of ZR after the vacuum test. The black curves are the default curves.

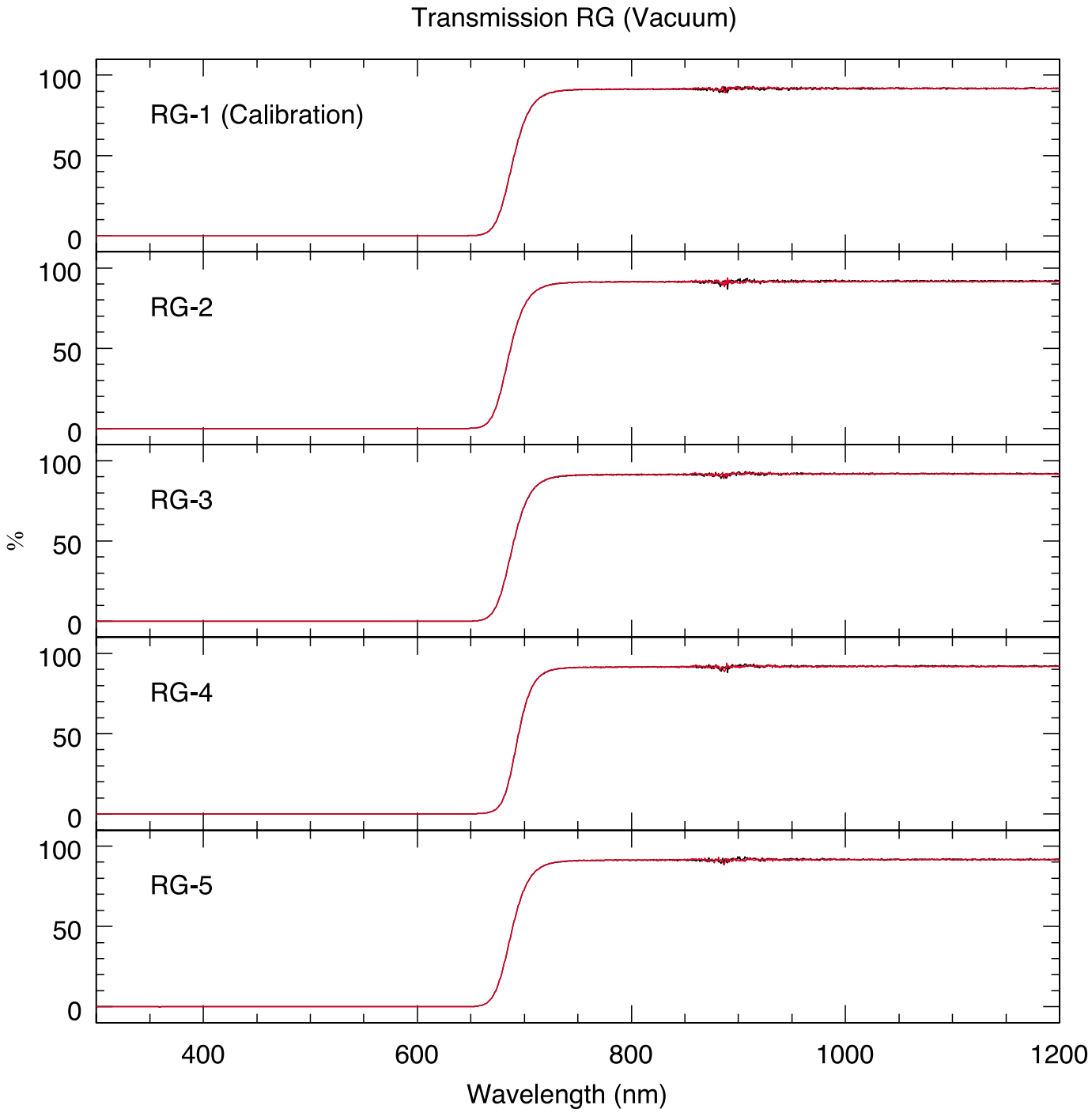

Figure 12: Transmission curves (red) of RG after the vacuum test. The black curves are the default curves.

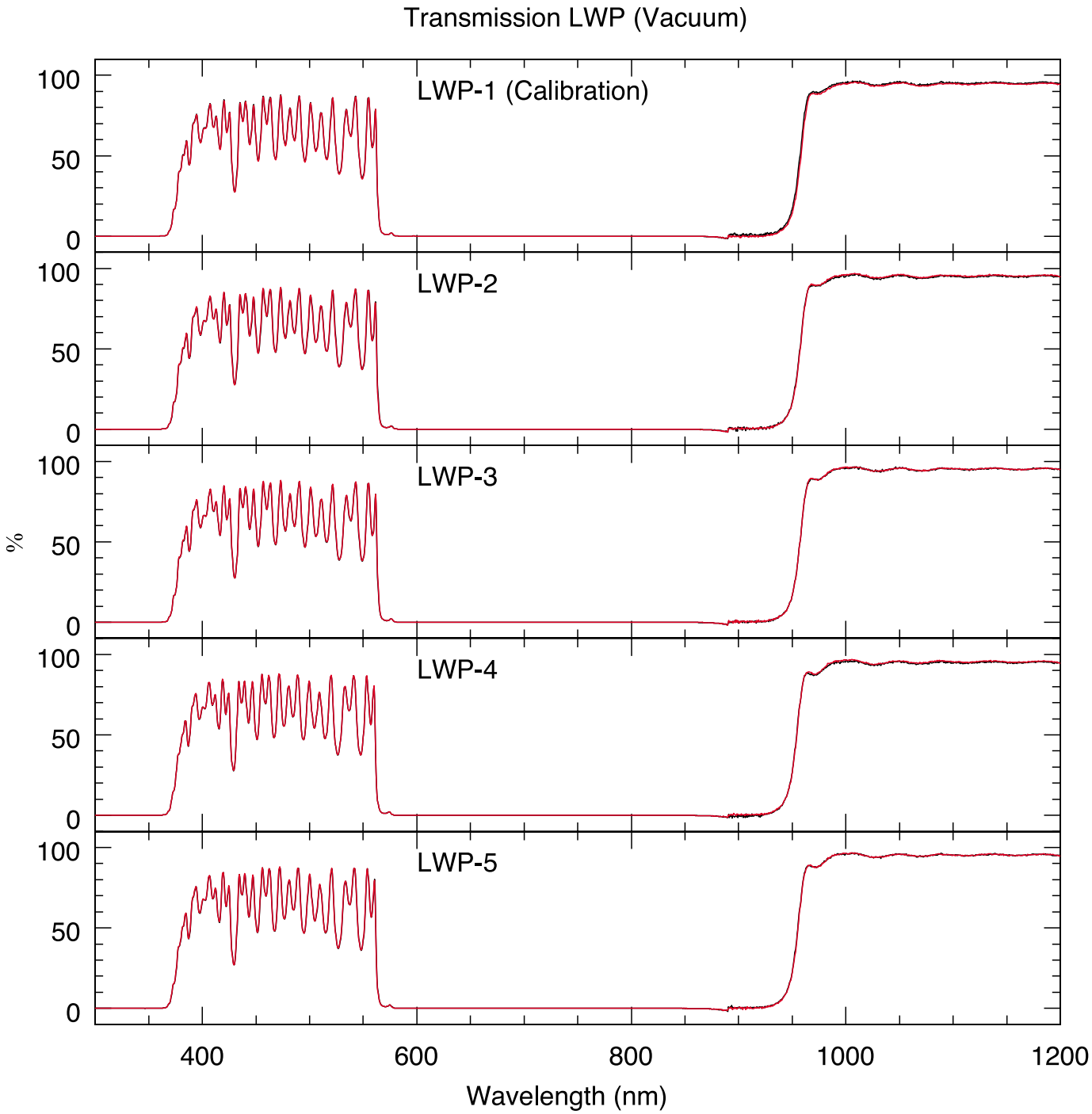

Figure 13: Transmission curves (red) of LWP after the vacuum test. The black curves are the default curves.

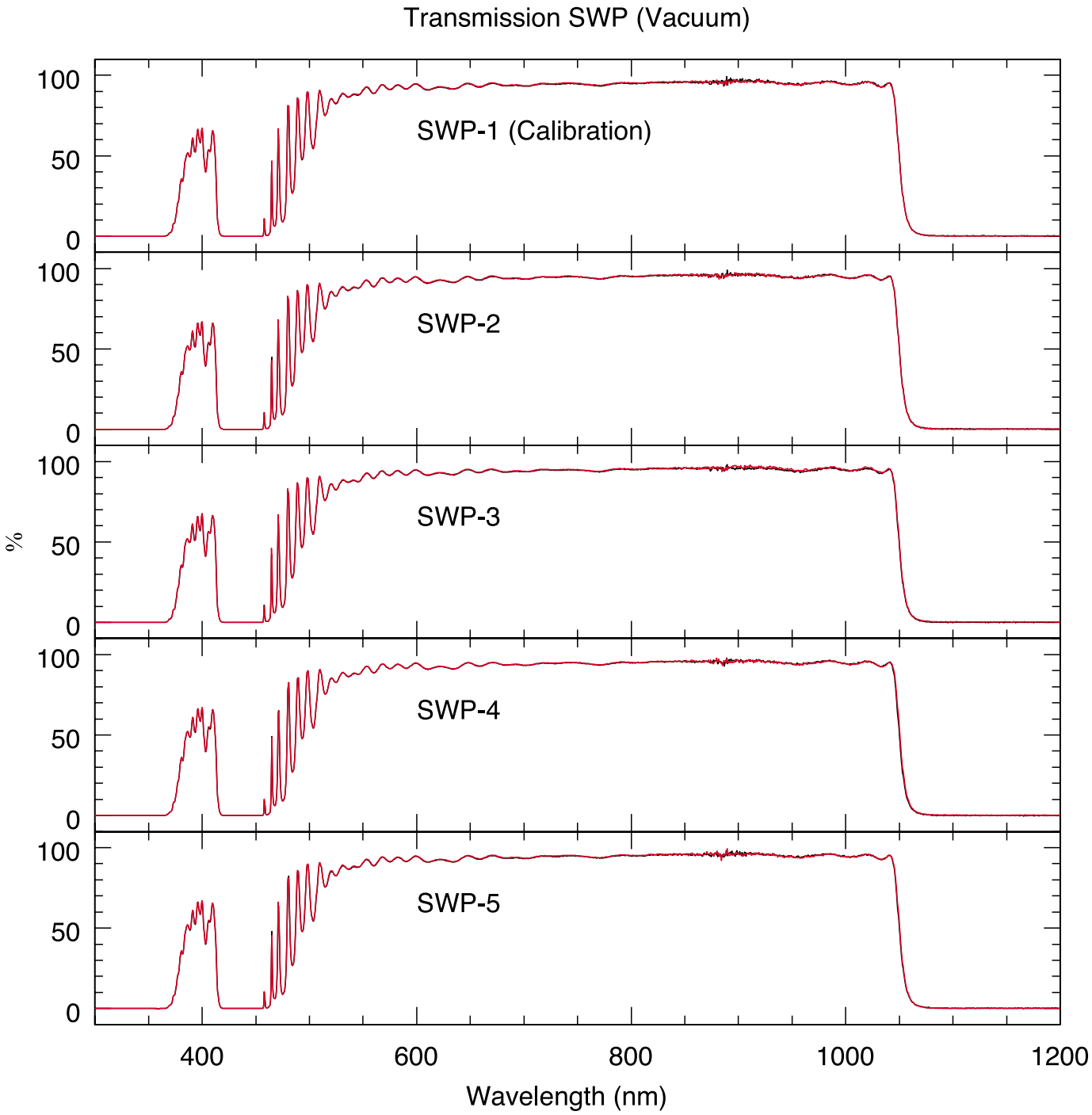

Figure 14: Transmission curves (red) of SWP after the vacuum test. The black curves are the default curves.

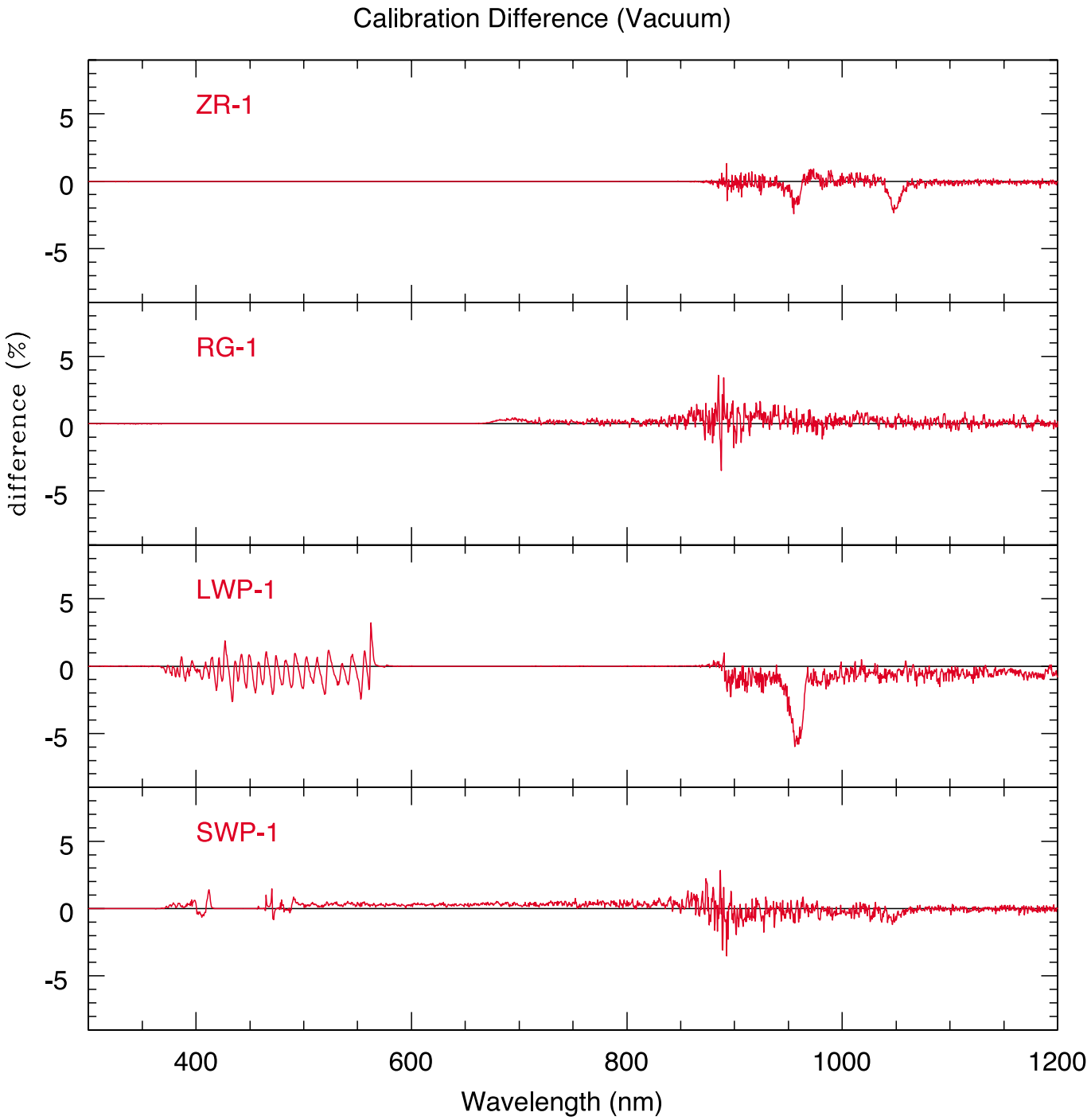

Figure 15: The difference obtained from the calibration measurement after the vacuum test.

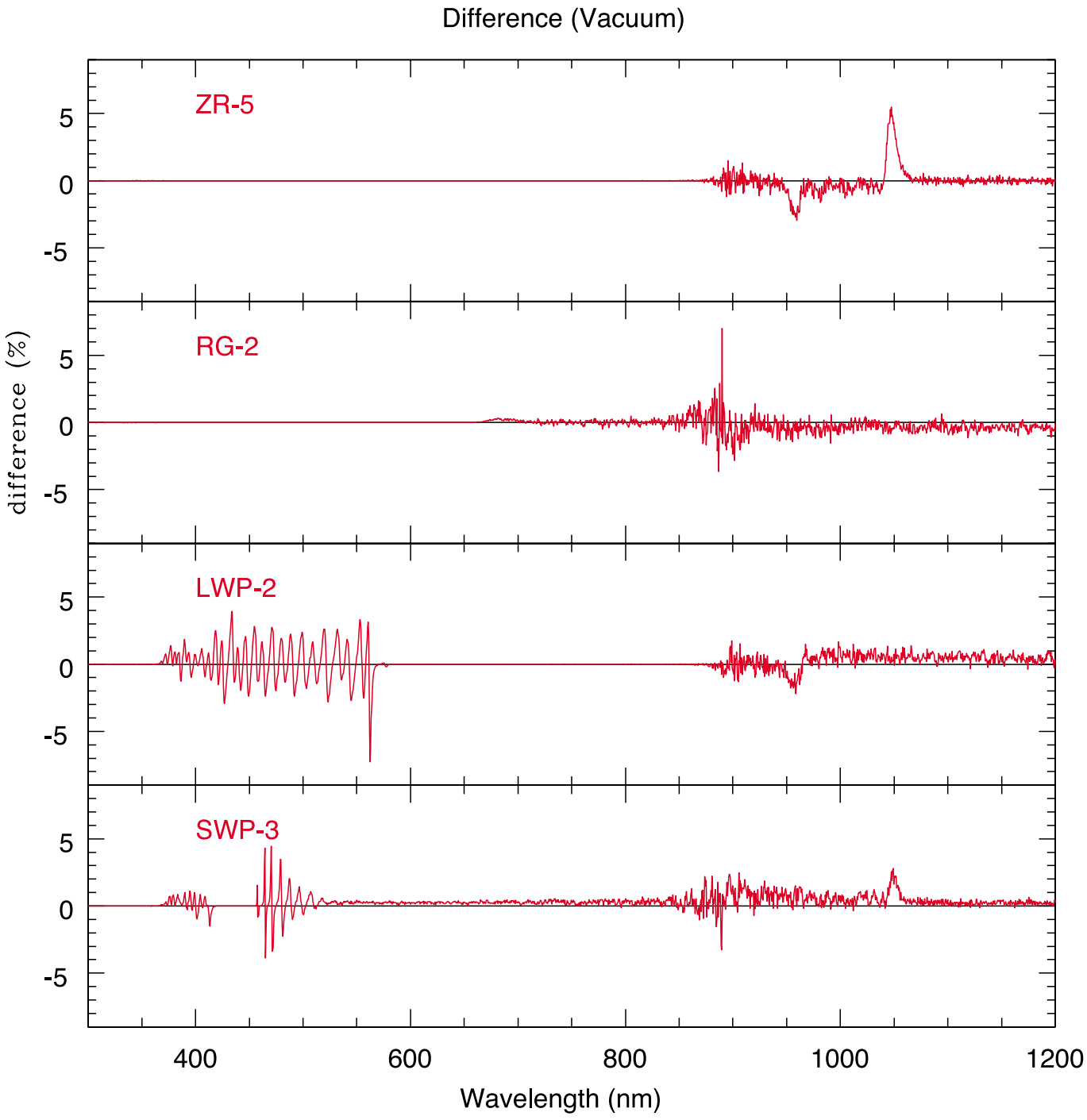

Figure 16: The largest difference between the default curve and the curve after the vacuum test.

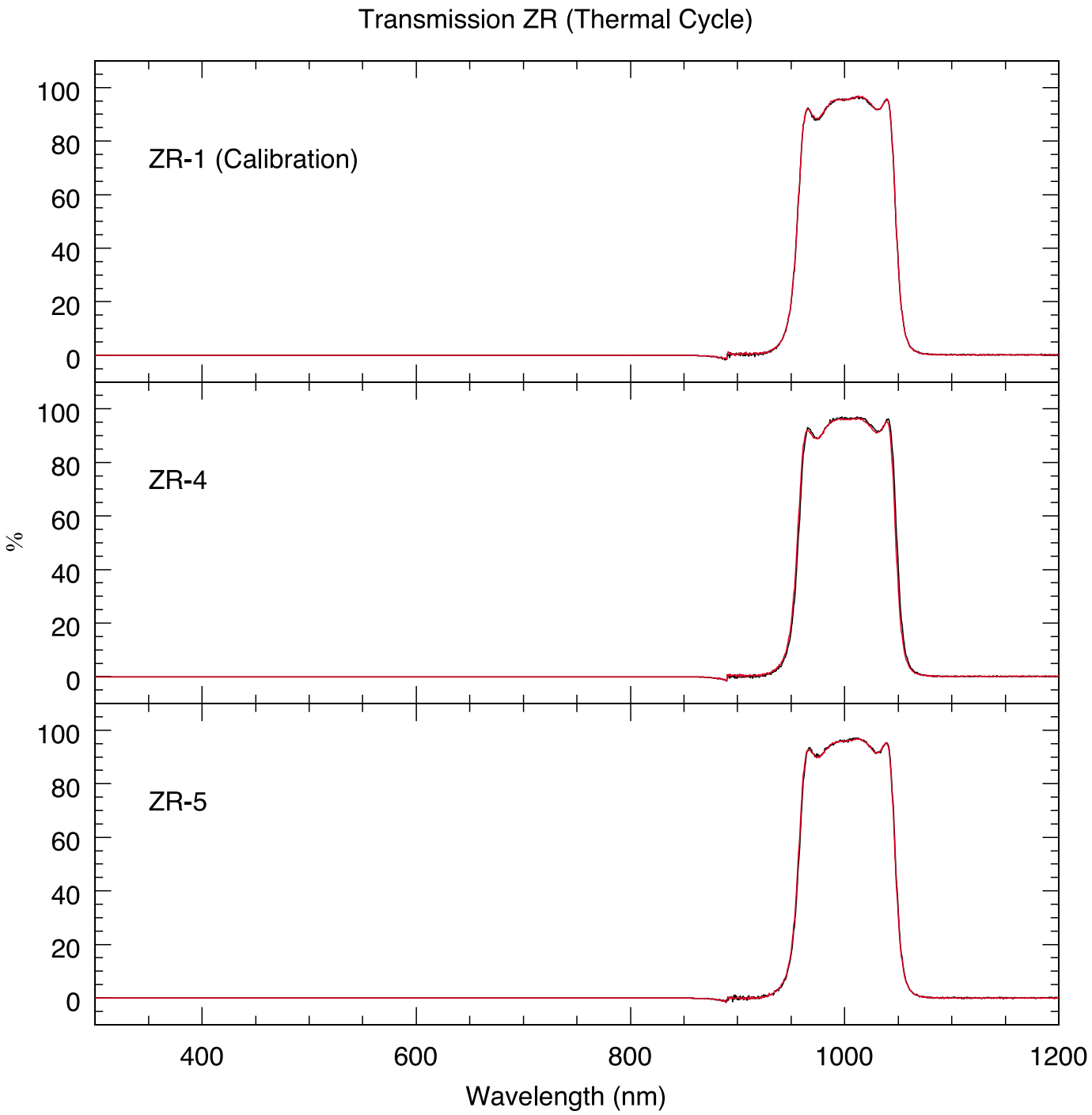

Figure 17: Transmission curves (red) of ZR after the thermal cycle test. The black curves are the default curves.

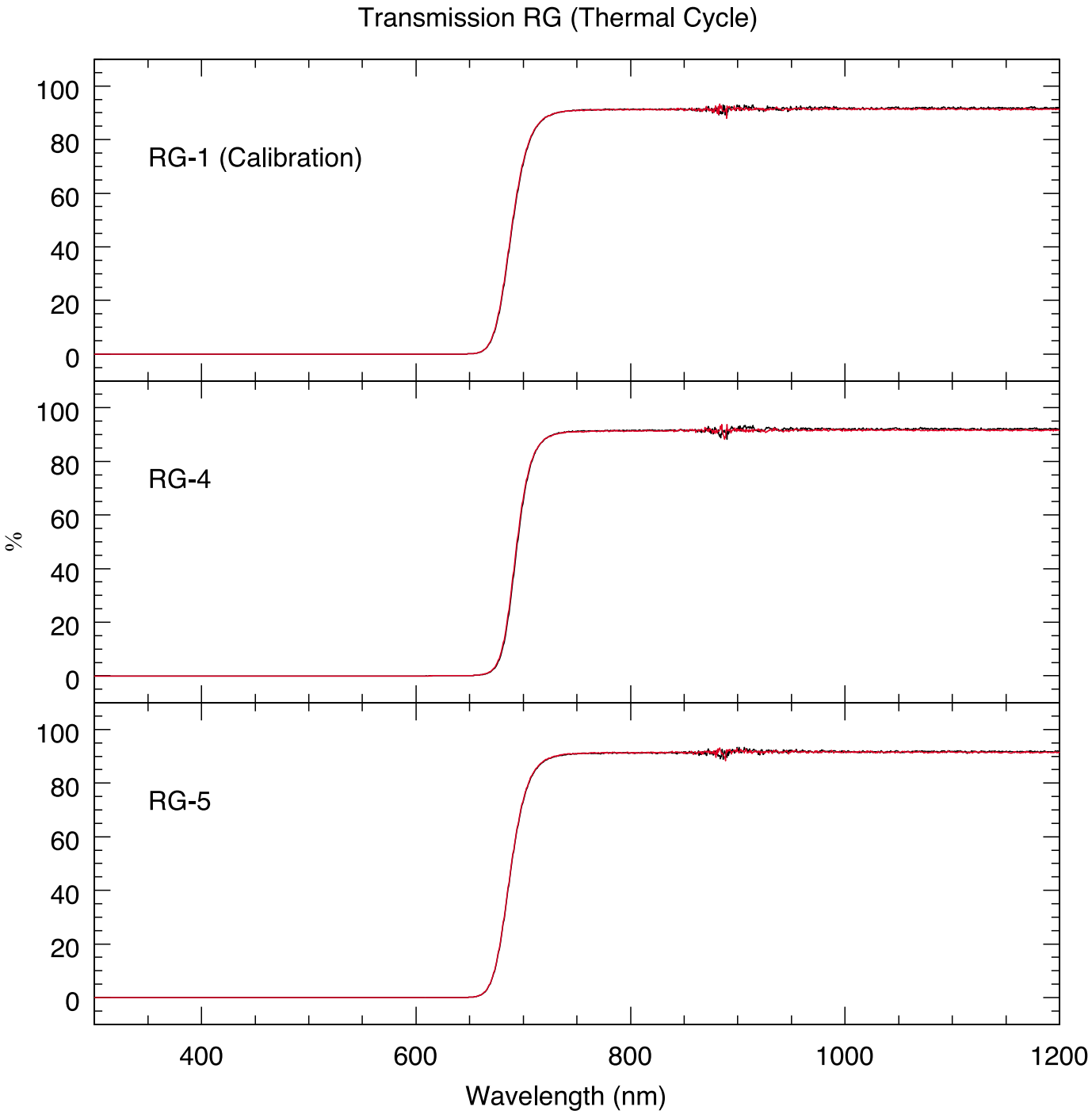

Figure 18: Transmission curves (red) of RG after the thermal cycle test. The black curves are the default curves.

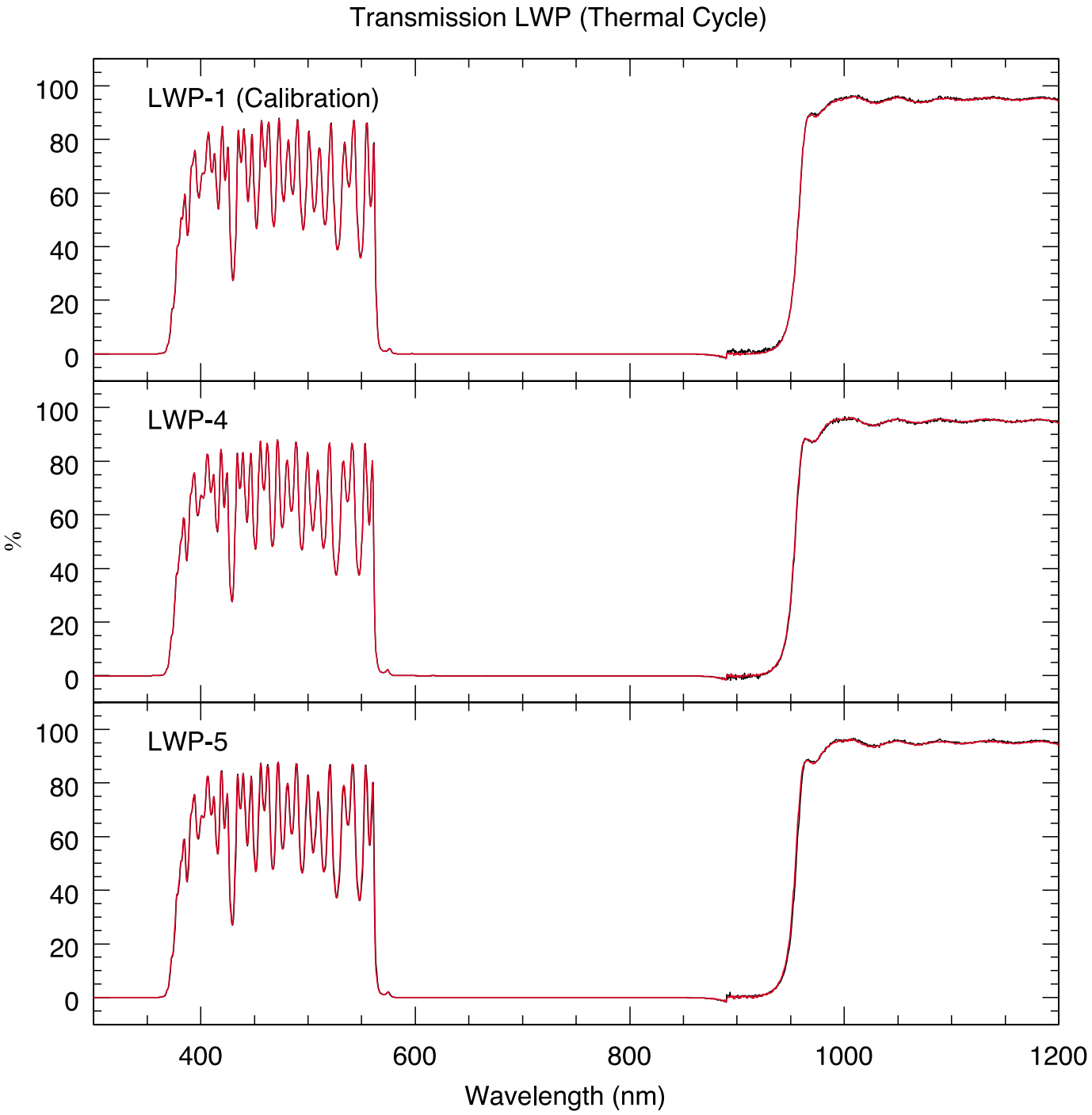

Figure 19: Transmission curves (red) of LWP after the thermal cycle test. The black curves are the default curves.

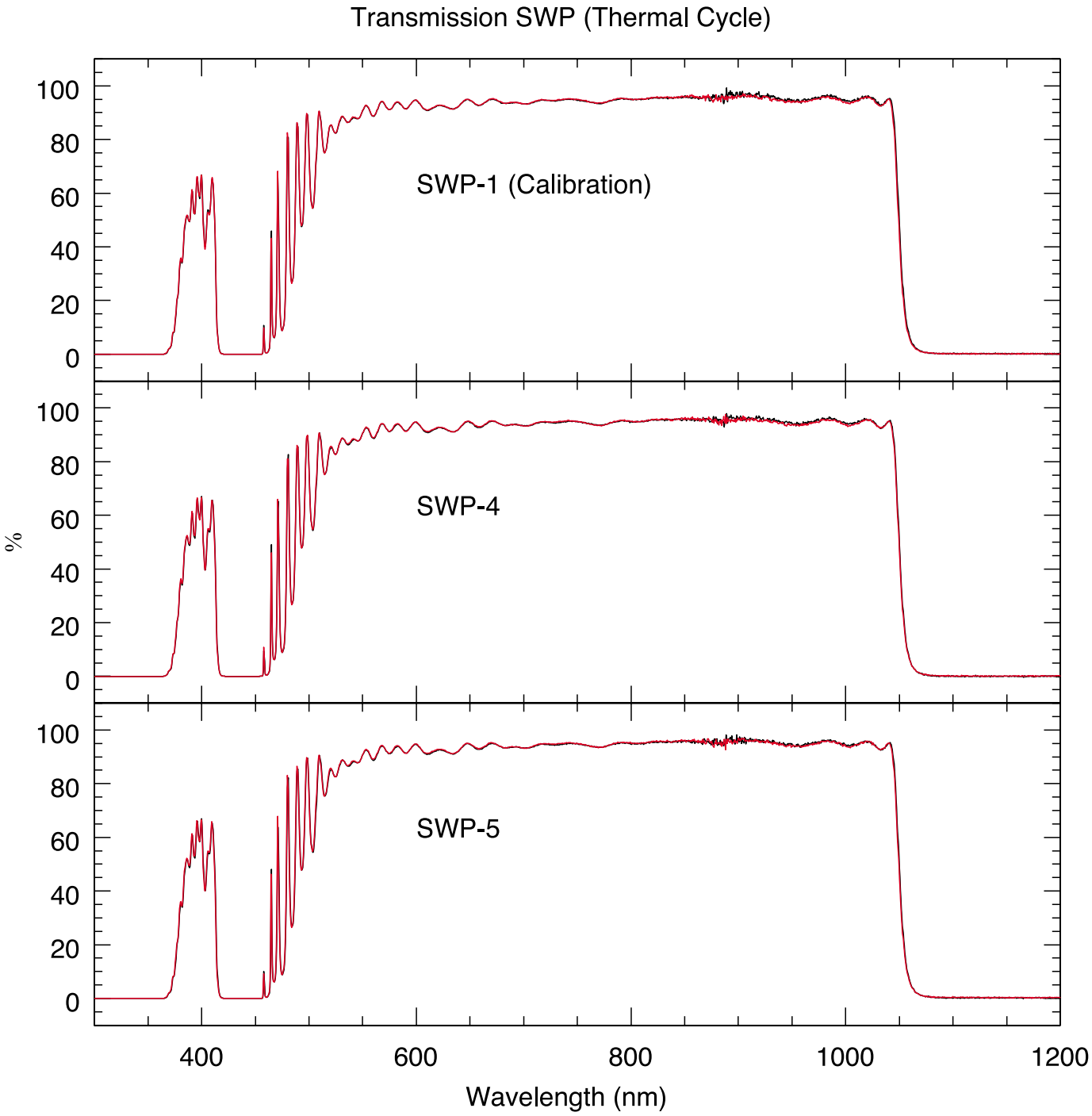

Figure 20: Transmission curves (red) of SWP after the thermal cycle test. The black curves are the default curves.

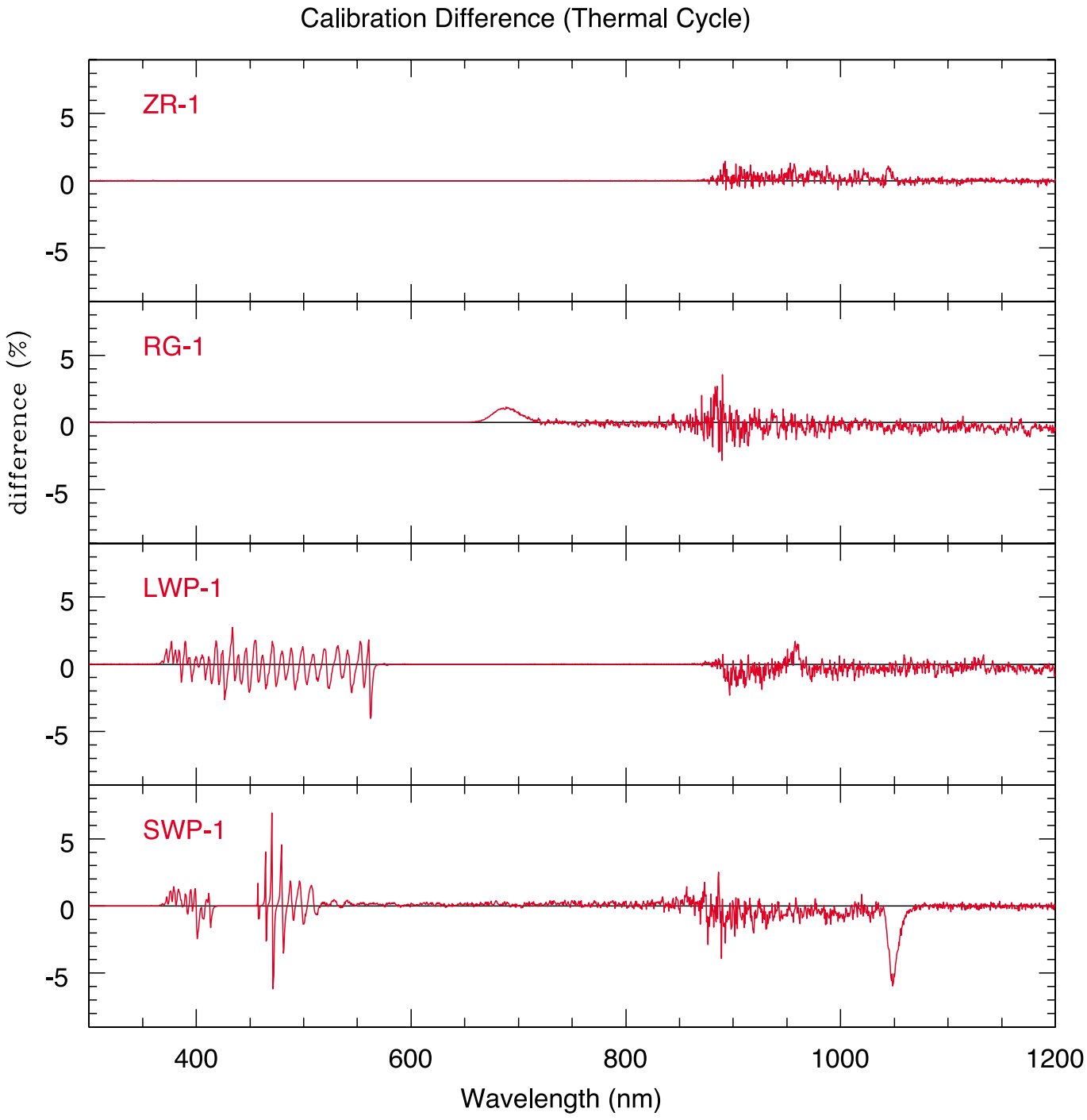

Figure 21: The difference obtained from the calibration measurement after the thermal cycle test.

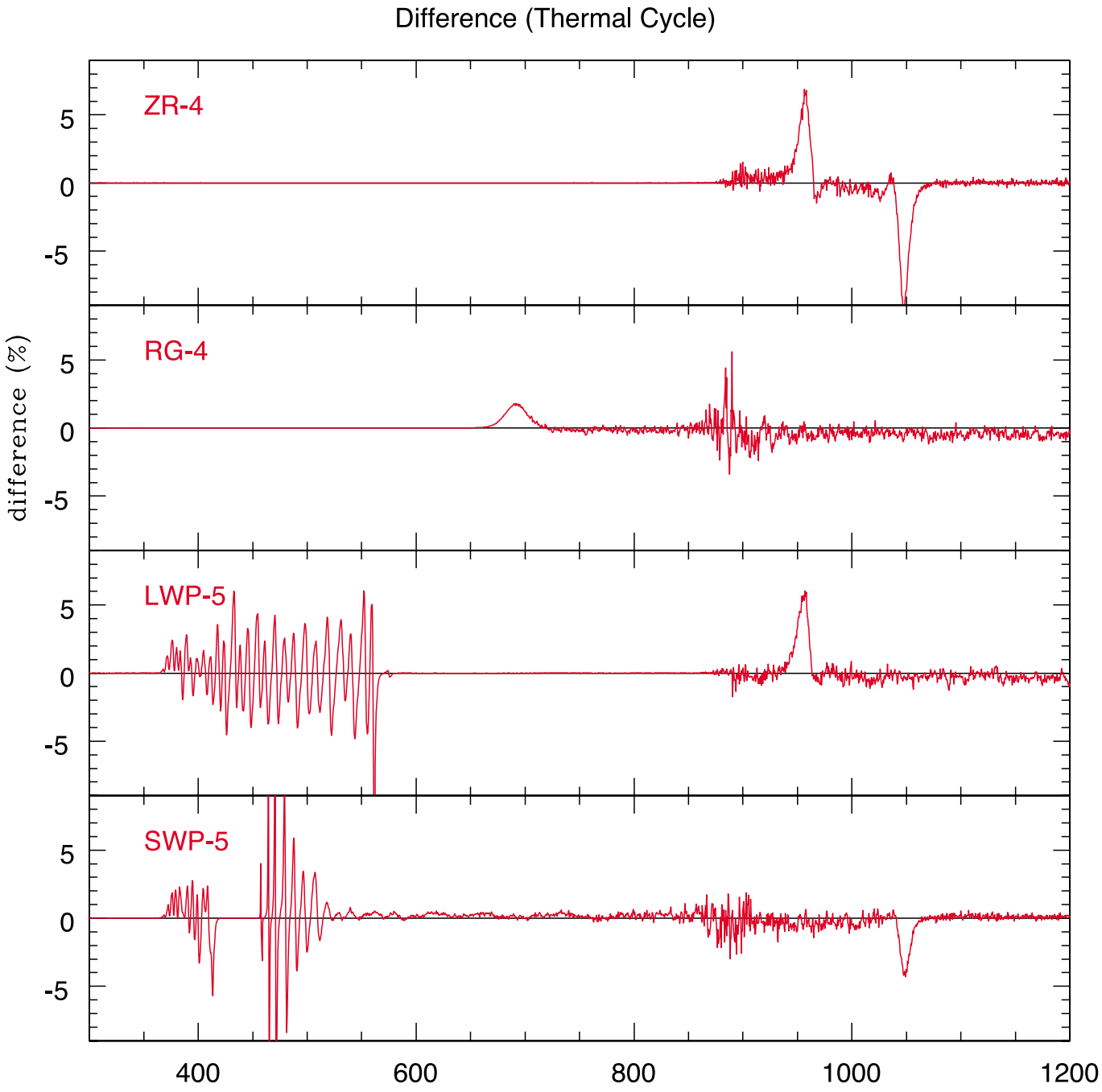

Figure 22: The largest difference between the default curve and the curve after the thermal cycle test.

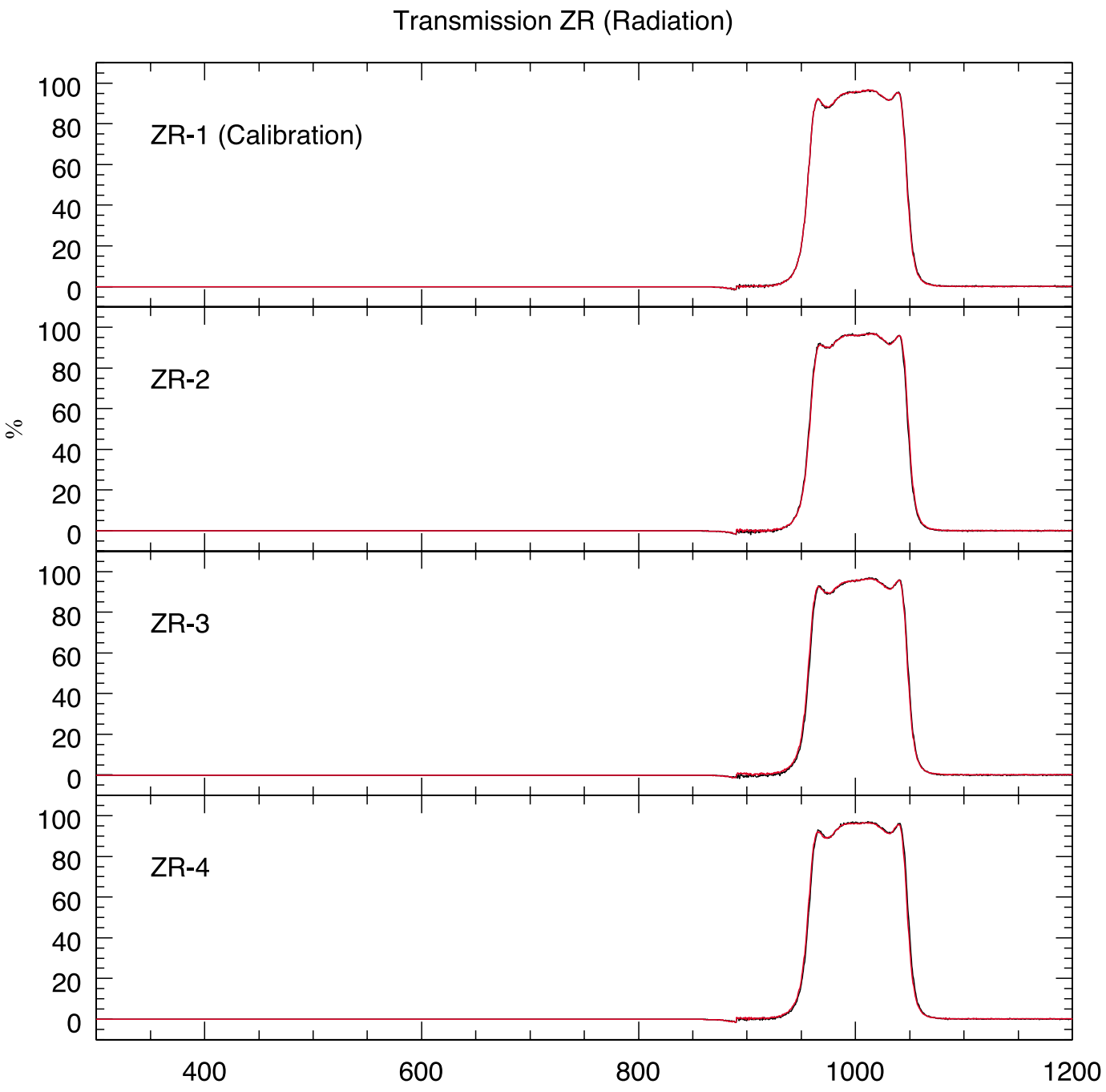

Figure 23: Transmission curves (red) of ZR after the radiation test. The black curves are the default curves.

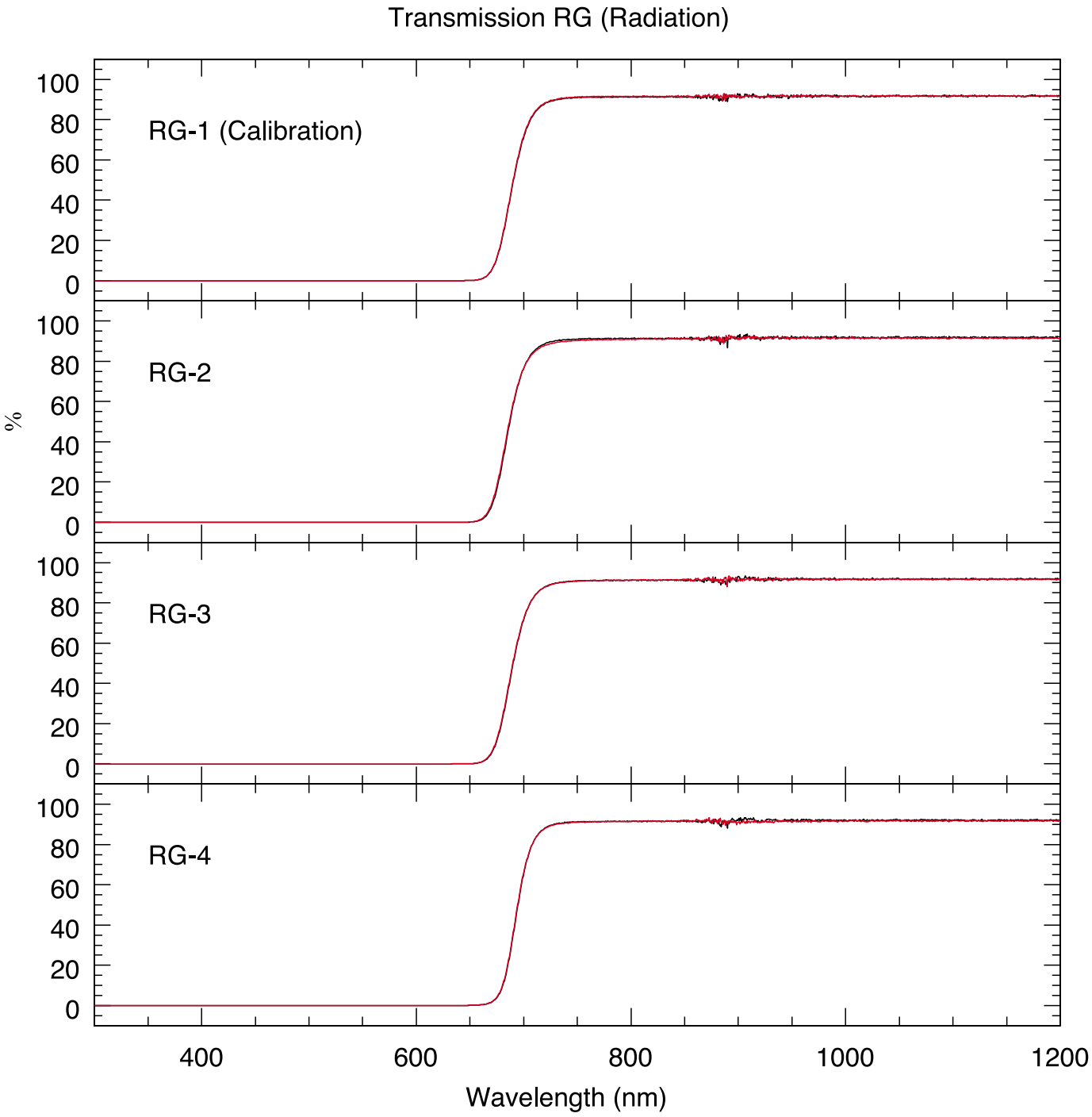

Figure 24: Transmission curves (red) of RG after the radiation test. The black curves are the default curves.

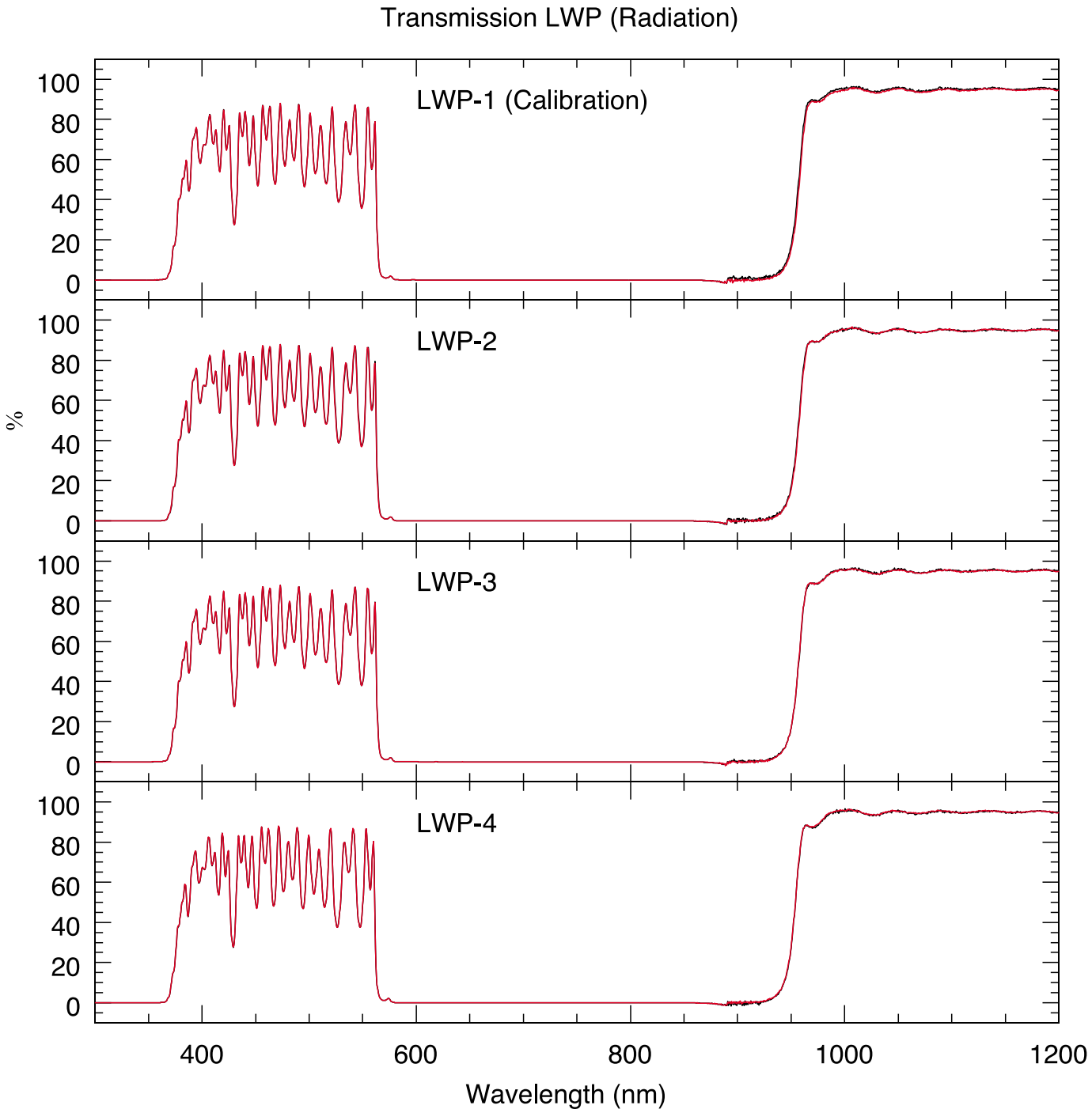

Figure 25: Transmission curves (red) of LWP after the radiation test. The black curves are the default curves.

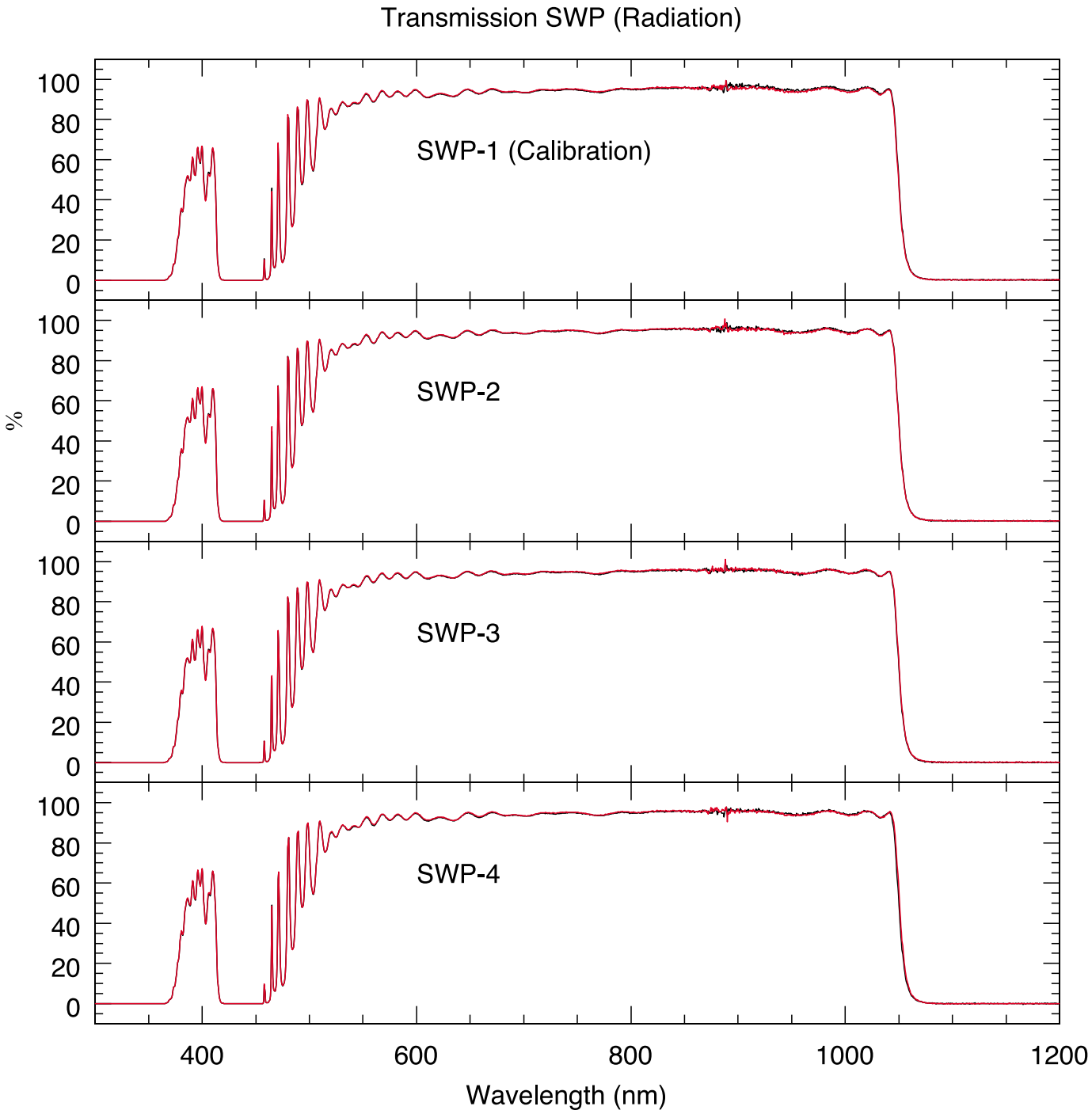

Figure 26: Transmission curves (red) of SWP after the radiation test. The black curves are the default curves.

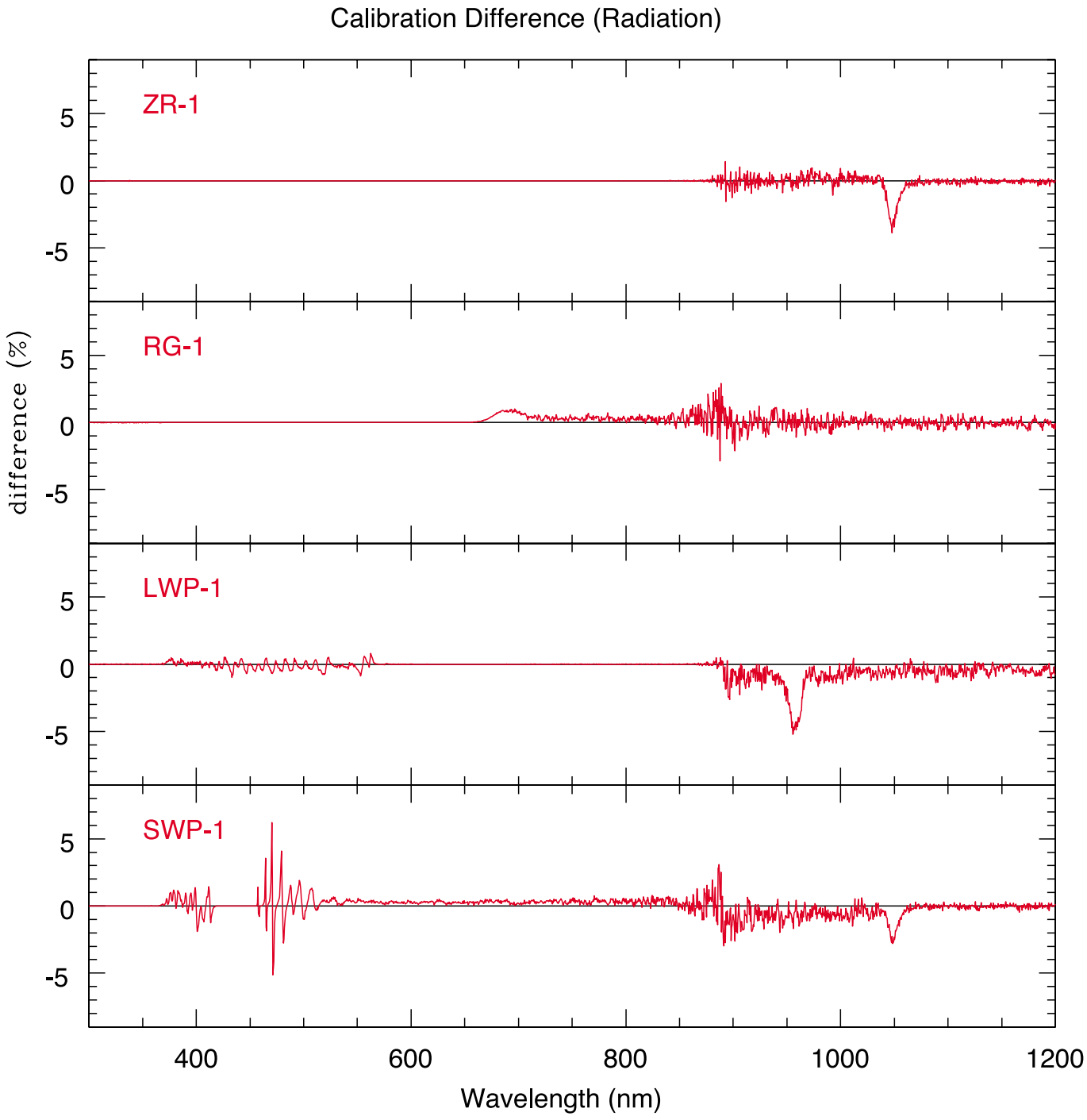

Figure 27: The difference obtained from the calibration measurement after the radiation test.

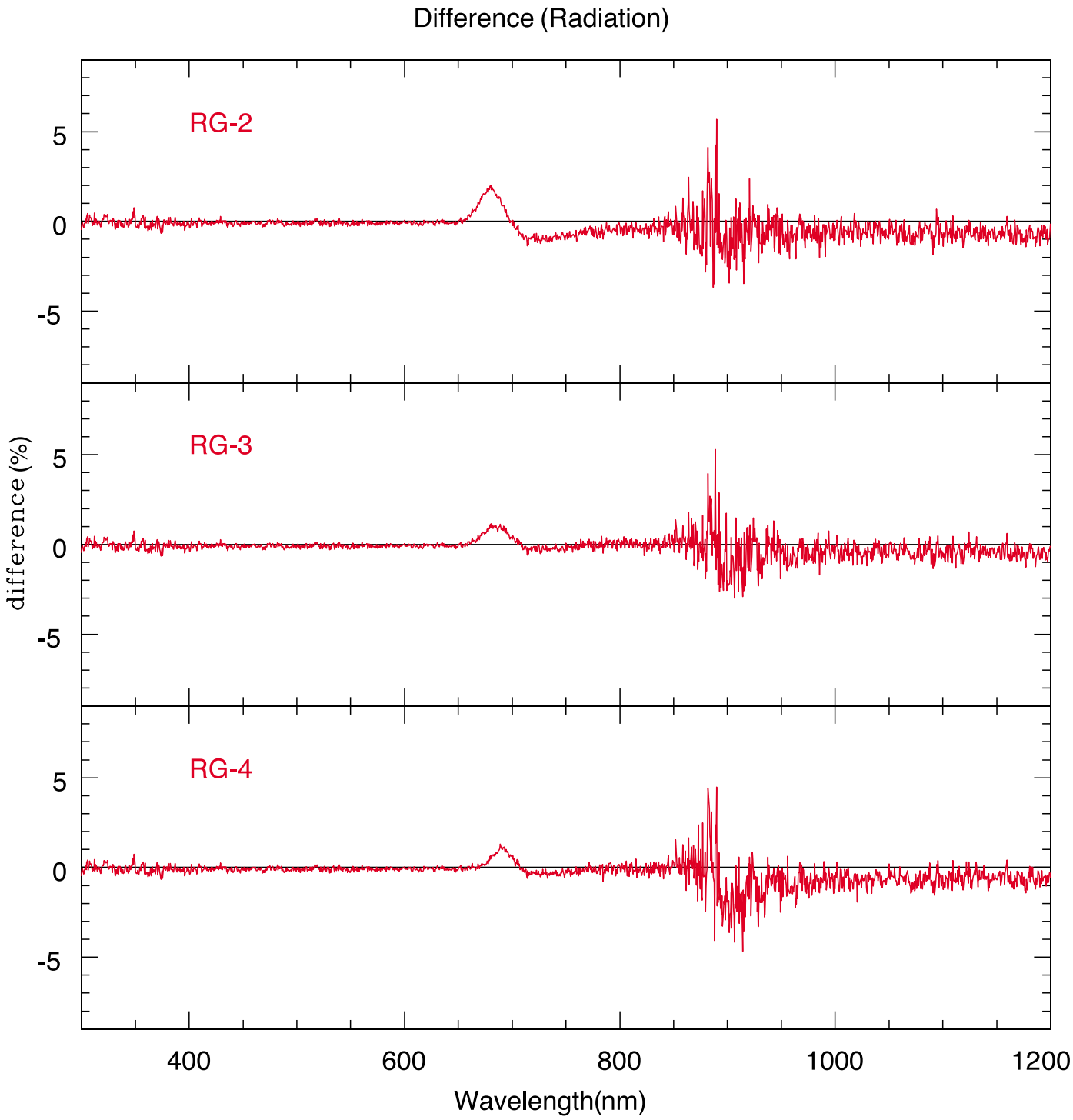

Figure 28: The difference between the default curve and the curve after the radiation test for RG.

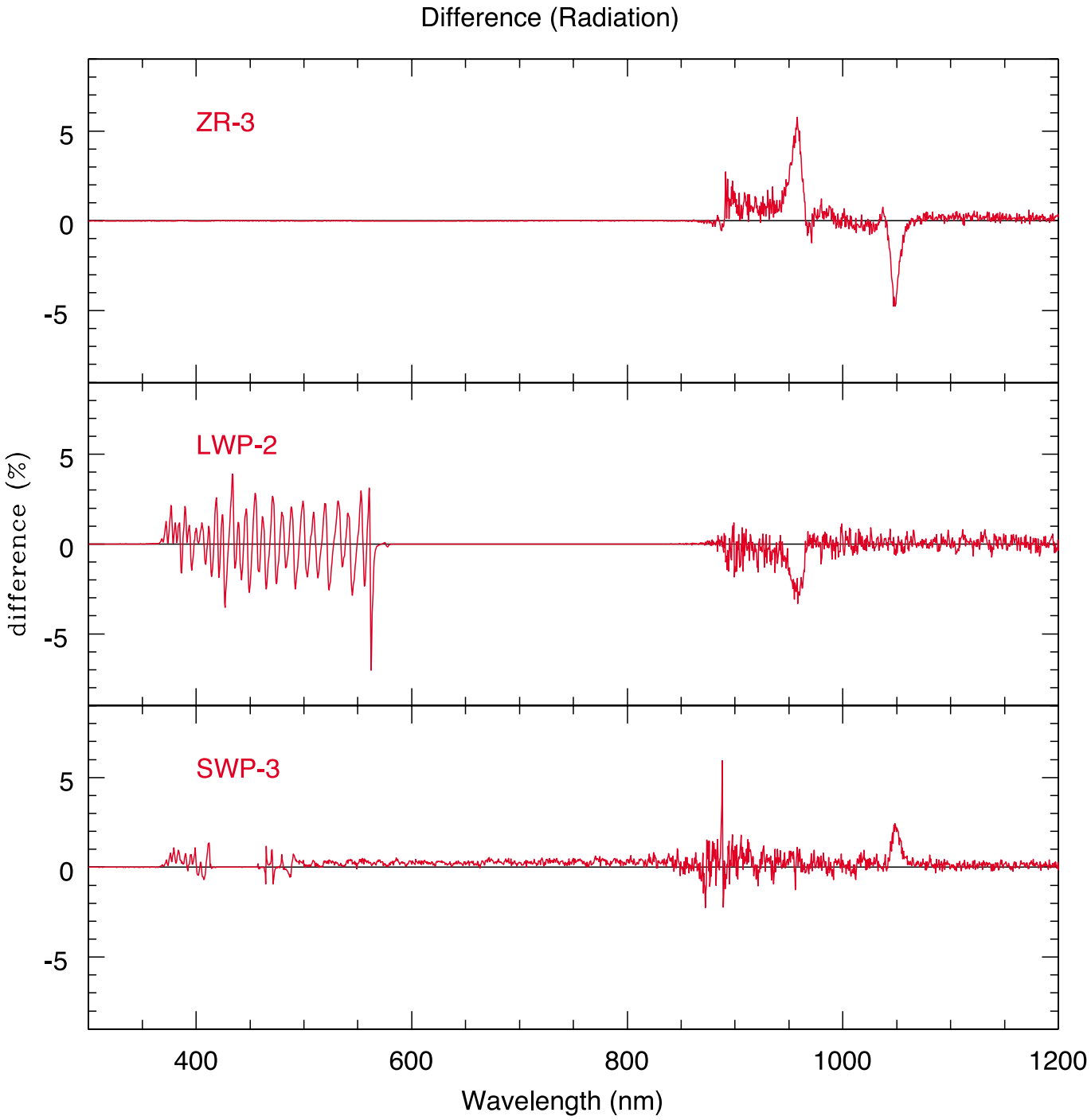

Figure 29: The largest difference between the default curve and the curve after the radiation test for ZR, LWP and SWP.